ABSTRACT

JOHNSTONE, STEPHANIE ELAINE. Uptake of a Fluorescently Labeled Alkamide by Mammalian Cells. (Under the direction of Dr. Scott Laster).

Alkamides are fatty acid amides produced by a variety of different plants. Alkamides exert immunomodulatory and anti-nociceptive effects and most studies of their mechanism of action have focused on the effects of alkamides on receptors and ion channels that mediate pain and inflammatory signaling. Whether alkamides can enter cells and potentially exert intracellular effects is unknown and will be the subject of this dissertation. To address this question, we produced a fluorescently labeled alkamide by replacing the isobutyl head group of the natural product (2E,4E)-N-isobutyldodeca-2,4-dienamide with a fluorescein (FITC) molecule. We found that this molecule (FITC-Alk) retained the ability to inhibit production of TNF-α from LPS-stimulated RAW 264.7 macrophage-like cells. Confocal microscopy was then used to characterize the entry and intracellular localization of FITC-Alk in RAW 264.7 cells. Our experiments revealed that the FITC-Alk entered cells within minutes and formed both large, bright puncta and diffuse pinpoint staining in the cytosol. Three-dimensional Z-stack depth coding revealed that puncta formation occurred throughout the cytoplasm in a uniform, non-polarized manner. The same pattern was seen also seen in Vero green monkey kidney cells and RBL-2H3 basophilic leukemia cells, suggesting a common pathway of uptake unrelated to the cell type or tissue of origin. Staining intensity was found to be both time and concentration dependent and continued linearly for at least 4 hours. Co-staining with Texas Red-dextran indicated that the large puncta produced by FITC-Alk uptake were intracellular endocytic compartments. Additionally, our data suggest a role for actin filaments in FITC-Alk uptake, and that the FITC-Alk molecule likely accumulates in Rab7

positive, late-stage endosomes. Intracellular proteins should therefore be considered as targets for alkamide activity and alkamides may be useful for endocytic drug targeting.

Uptake of a Fluorescently Labeled Alkamide by Mammalian Cells

by
Stephanie Elaine Johnstone

A dissertation submitted to the Graduate Faculty of
North Carolina State University
in partial fulfillment of the
requirements for the degree of
Doctor of Philosophy

Microbiology

Raleigh, North Carolina
2021

APPROVED BY:

Scott M. Laster, Ph.D. Committee Chair	Michael Sikes, Ph.D.
Frank Scholle, Ph.D.	Santosh Mishra, Ph.D.

BIOGRAPHY

Stephanie Elaine Johnstone was born to Kathleen and Robert Johnstone and raised in Morgantown, West Virginia along with her two sisters, Erica and Emily. She grew up looking at the pictures in her father's medicine journals and always knew she wanted to be in biomedicine. She started her research career at the National Institute of Health's National Institute of Environmental Health Sciences as a summer research intern and fell in love with research. The following year she started work in the laboratory of Dr. Art Frampton at the University of North Carolina Wilmington as an undergraduate researcher. She stayed in Dr. Frampton's lab and earned a Bachelor of Science in biology and Master of Science in biology in 2013 and 2015, respectively.

Upon completing her MS degree, she volunteered as a teacher's aide in the Science Department at Durham Academy Lower School while she applied to doctoral programs. She joined the microbiology graduate program at North Carolina State University in Fall 2016, and Dr. Scott Laster's lab shortly thereafter. During her time at North Carolina State University, Stephanie won two back-to-back Graduate Student Association Teaching Awards for Excellence in Laboratory Teaching, as well as a seed grant from the Emerging and Infectious Disease group within the Comparative Medicine Institute. Under the direction of Dr. Laster, Stephanie studied the uptake and function of alkamides from *Echinacea*. Much of the details of her work are included herein.

ACKNOWLEDGMENTS

First and foremost, I would like to thank my advisor, Dr. Scott Laster, for allowing me to grow as a scientist and gain confidence in academic research and professional skills. He has been a constant source of support and knowledge, and I will always value my time training with him. I also want to thank my committee members, Dr. Michael Sikes, Dr. Frank Scholle, Dr. Santosh Mishra, and Dr. Joshua Pierce for their guidance and encouragement over the years. I have learned a lot and they have always been available to help and drive my research forward. I also want to acknowledge and thank my immunology journal club peers and the participating professors who have taught me to think critically about research and always look for the overall question.

Additionally, I want to thank my family who have literally supported me throughout this endeavor and allowed me to follow my dreams of earning a PhD. I also want to thank my wonderful, brilliant partner who has always been there to help take care of anything I've needed. And finally, I want to thank my friends and fellow graduate students, Jace Natzke and Hunter Whittington. You two are the best and with who I hold some of my best graduate school memories.

TABLE OF CONTENTS

LIST OF FIGURES

CHAPTER 1: LITERATURE REVIEW

1.1. Introduction

Plants came into use as medicines by humans before writing appeared with some experts estimating that the use of medicinal plants began 60,000 years ago at the time of the Neanderthals (Ji, Li, & Zhang, 2009). Even in the 21st century, 11% of the 252 drugs considered essential by the WHO are still prepared from plants, such as morphine from the opium poppy (*Papaver somniferum*) and digoxin from foxglove (*Digitalis purpurea*) (Patil et al., 2012; Ziegler, Diaz-Chávez, Kramell, Ammer, & Kutchan, 2005). Researchers skilled in synthetic and computational chemistry routinely use compounds from medicinal plants as a starting point in drug development. Paclitaxel, for example, is derived by semi-synthesis from 10-deacetylbaccatin found in the European yew (*Taxus baccata*), while artemether is also produced by semi-synthesis from artemisinin found in sweet wormwood (*Artemisia annua*) (Ghassempour et al., 2007; Shinde, Sebastian, Jain, Hanamanthagouda, & Murthy, 2016). Plant-derived compounds are used extensively in both modern and traditional medicine and will be the subject of this dissertation.

1.2. The alkamides

One class of plant-derived bioactive compounds are the alkamides, also referred to as alkylamides. Alkamides are fatty acid amides which vary in structure and function. The structure of a prototypical alkamide is shown in **Fig. 1.1**. Alkamides contain a fatty acid tail which can vary in the number of carbons and the presence/absence of unsaturations, an amide group, and a variable headgroup, such as an isobutyl group as shown in the alkamide dodeca-2E,4E-dienoic acid isobutylamide below. This alkamide is also known as A15 (for its retention time from a silica gel column) and will be the focus of this report (**Figure 1.1**).

Figure 1.1 B-E also shows the structure of several other alkamides that have been studied extensively. Spilanthol, which is found in many plants, including several species in the *Acmella* and *Spilanthes* genera and *Heliopsis longipes*, has 10 carbons and three double bonds in the fatty acid region (**Figure 1.1 B**). Spilanthol has been used historically in several ways, with the most common usage as an analgesic. Plants containing spilanthol are often called "toothache plants" where the plant matter is chewed, causing a local numbing sensation in the mouth (Barbosa et al., 2017). Pellitorine, found in plants from the *Piper* genus, is similar to A15 with double bonds positioned at two and four carbons, an isobutyl headgroup, but with only a 10-carbon fatty acid chain (**Figure 1.1 C**). Sanshool, shown here as hydroxy-α-sanshool, is found in plants in the *Zanthoxylum* genus which includes the Szechuan peppercorn (**Figure 1.1 D**). Sanshool contains 12 carbons with multiple double bonds in the fatty acid chain and a hydroxyl group in the headgroup. A number of analogs of sanshool have been identified with hydroxy-α-sanshool believed to be the major bioactive compound in most plant extracts (Bautista et al., 2008). Also shown in **Figure 1.1** is capsaicin, which contains a nine carbon fatty acid, with a methyl group in the fatty acid chain and an unsaturation at the sixth carbon (**Figure 1.1 E**). Capsaicin also contains an aromatic head group, and through its ability to activate the TRPV-1 receptor, is responsible for the painful sensation associated with "hot peppers" (O'Neill et al., 2012).

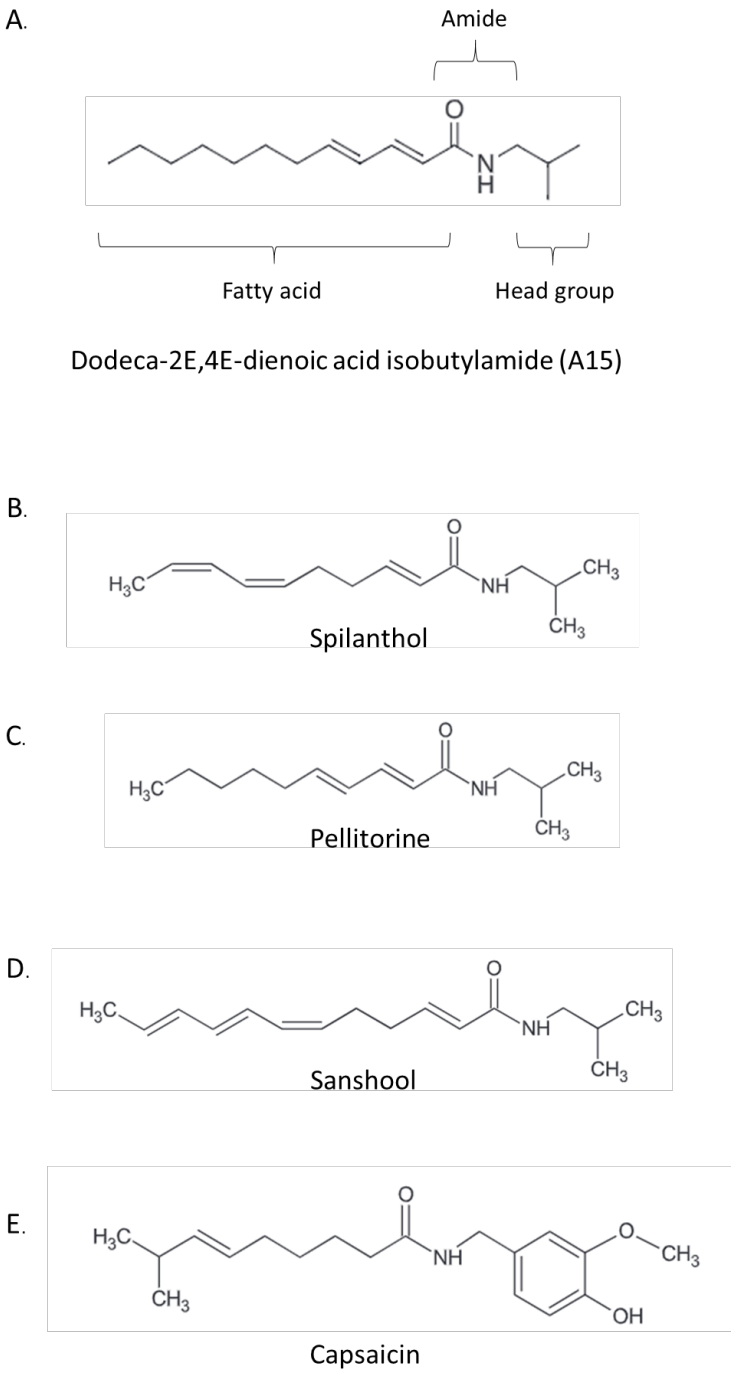

Figure 1.1. General structure of alkamides. A. Dodeca-2E,4E-dienoic acid isobutylamide (A15) is shown above as a representation for the general alkamide structure. Other alkamides from *Acmella/Spilanthes* (spilanthol) (B), *Piper nigrum* (pellitorine) (C), *Zanthoxylum* (sanshool) (D), and *Capsicum* (capsaicin) (E). Structures B-E taken from Boonen et al 2012.

1.3 Alkamides in Traditional Medicine

1.3.1 ***Echinacea.*** Alkamides occur in the flowering plants of the *Echinacea* genus, including the species *purpurea*, *angustifolia*, and *pallida* (Stuart & Wills, 2000). Alkamide containing *Echinacea* extracts have been used historically by a variety of peoples including numerous Native American tribes for a wide range of purposes including treatment of infected wounds, rabies, or painful conditions such as toothaches or snakebites (Kindscher, 2016). In 1805, Lewis and Clark learned about the use of this medicinal plant on their famous expedition and mailed seeds and roots to President Jefferson noting it as one of their important finds (Kindscher, 2016). Today, *Echinacea* extracts are used to treat a variety of conditions- most often the common cold, but also bronchitis, upper respiratory infections, and more generally as an anti-inflammatory (Parsons, Cameron, Harris, & Smith, 2018; Percival, 2000). Recently, the role of the alkamides in the uses for *Echinacea* have been studied by a number of labs.

Alkamides from *Echinacea,* such as A15, have been shown to act on a variety of cell types, including many immune cells such as macrophages, mast cells, and T cells, and also neurons (Gerhold & Bautista, 2010; Travis V. Gulledge et al., 2018; Todd et al., 2015). In immune cells, A15 suppresses activation of pro-inflammatory responses such as production of pro-inflammatory cytokines and chemokines, which may account for the reduction of symptoms when *Echinacea* is used to treat respiratory infections (Todd et al., 2015). In addition to the modulation of important inflammatory cytokines, alkamides from *Echinacea* are useful in inhibiting activation of mast cells and T cells, which has been linked to the inhibition of calcium-dependent signaling (Travis V. Gulledge et al., 2018). In neurons, alkamides have been shown to block ion channel activity leading to analgesia, which further reinforces their use to relieve symptoms caused by the common cold or respiratory infections (Gerhold & Bautista, 2010). *Echinacea* extracts have also been tested

successfully in clinical trials to treat eczema where a significant reduction in local inflammation was noted (Oláh et al., 2017).

1.3.2 ***Piper longum & Piper nigrum*.** Plants containing alkamides have not only been used by Native Americans, but they have also been used by people around the globe in China, Mexico, Brazil, Africa, Europe, and India (Elufioye, 2020). *Piper* species, such as the long pepper, have been used in traditional medicine to treat a range of conditions such as chronic bronchitis, asthma, viral infections, and diarrhea and their use first appeared in texts by Hippocrates (S. Kumar, Kamboj, Suman, & Sharma, 2011). The plant *Piper longum* L., which contains 16 known alkamides, has been used to treat stomach conditions in ancient Chinese medicine and in traditional Indian medicine to treat abdominal pain and disease, among other diseases and disorders (Abdubakiev, Li, Lu, Li, & Aisa, 2020; Yadav, Krishnan, & Vohora, 2020). Modern research has shown that these alkamides can increase melanin content and tyrosinase activity in melanoma cells (Abdubakiev et al., 2020) leading to suggestions that *Piper* extracts might produce an anti-melanoma affect. In addition, pellitorine displayed a strong cytotoxic activity in a study with two tumor-derived cell lines (Ee, Lim, Rahmani, Shaari, & Bong, 2010). Alkamides isolated from *Piper longum* have also been shown to suppress NF-κB activation and inhibit the activity of COX-1 and -2 (Y. Liu, Yadev, Aggarwal, & Nair, 2010). Inhibition of prostaglandin synthesis was also observed in ionophore stimulated leukocytes treated with pellitorine containing *Piper* extracts (Stöhr, Xiao, & Bauer, 2001). Finally, pellitorine has also been shown to be an effective insecticidal agent against the housefly and *Aedes aegypti* mosquito (Miyakado, Nakayama, Yoshioka, & Nakatani, 1979; Park, 2012).

1.3.3. *Phyllanthus*. Traditional healers in India have used the plant *Phyllanthus fraternus* to treat liver disorders, mixing the plant into a paste or using plant extract (Ghatapanadi et al 2011). Aqueous extracts from the plant, which are used by Indian healers, possess antioxidant activity and can prevent the oxidation of lipids and proteins (Rios Gomez 2012). In isolated hepatocyte mitochondria, the extracts are protective against alcohol induced oxidative stress (Sailaja & Setty, 2006). *Phyllanthus sp.* have also been used in Ghana as an anti-malarial treatment and two alkamides E,E-2,4-octadienamide and E,Z-2,4-decadienamide (both of which lack the alkyl residue on the amine group) are thought to contribute to it's anti-malarial activity (Sittie et al 1998).

1.3.4 *Spilanthes*. In Mexico, alkamide containing *Spilanthes* plants have been used as insecticides as well as analgesics (Molinatorres, Salgado-Garciglia, Ramirez-Chavez, & Del Rio, 1996). In Africa and India, *Spilanthes acmella* is used as an medication to treat malaria (Spelman, Depoix, McCray, Mouray, & Grellier, 2011). In regions of Brazil, extracts from these plants have also been used as a female aphrodisiac (de Souza et al., 2019). Spilanthol is the predominant alkamide found in *Spilanthes sp.* with several other alkamides reported in lesser quantities (Paulraj, Govindarajan, & Palpu, 2013). Commercial preparations of spilanthol are as available for use as oral analgesics and to provide a long-lasting mint flavor in toothpastes (Barbosa et al., 2017). In animal models, analgesia was demonstrated using a *Spilanthes* extract and was found to reduce hind paw edema and acetic acid induced tail flick in a dose dependent manner (Dubey, Maity, Singh, Saraf, & Saha, 2013). Spilanthol displays structural similarities to capsaicin (**Fig 1.1**), the ligand for the nociceptor transient receptor potential (TRP) channel TRPV1, which may account for its analgesic properties (Rios and Olivo 2014). Isolated spilanthol also displays immunomodulatory properties *in vitro* causing dose dependent reduction in macrophage activation and nitric oxide (NO)

production, as well as inhibition of cytokine production and NF-κB activation (Wu et al., 2008). Other uses for spilanthol have been investigated including as an antipyretic, antimicrobial, antifungal, diuretic, and vasorelaxant (Prachayasittikul, Prachayasittikul, Ruchirawat, & Prachayasittikul, 2013).

1.3.5. *Zanthoxylum clava-herculis*. *Zanthoxylum clava-herculis,* also known as the toothache tree, Hercules' club, or prickly ash, has been used as a medical plant by Native Americans. In East Asia this plant is used as an analgesic, an antimicrobial, and for the treatment of kidney and liver disorders (Pawlus et al.; Steinberg, Satyal, & Setzer, 2017). For example, extracts from the bark of *Zanthoxylum* display antimicrobial activity against Gram negative and Gram positive bacteria, and yeast *in vitro* (Pilna et al., 2015). Several alkamides have been isolated from *Zanthoxylum clava-herculis* including α-sanshool, and the presence of these molecules may explain the activities of this plant (Pawlus et al.) The alkamides in *Zanthoxylum clava-herculis* extracts have been shown to bind cannabinoid receptors, perhaps suggesting the mechanism of analgesic action (Cieśla & Moaddel, 2016).

1.3.6. Other plants. Alkamides have been identified from a variety of other plants representing over 30 different plant families (Rios 2012). A few come from the *Solanaceae* family such as *Capsicum annuum* L. which has been used to treat otitis, infections, rheumatism, and headache (Boonen et al., 2012). Alkamides have also been identified in another plant from the same family, *Nicotiana tabacum* L., which is used in Africa to treat convulsions and as a stimulant (Boonen et al., 2012). Extracts of *Ricinus communis* L., which is a member of the *Euphorbiaceae* family, contains alkamides and is used by Mediterranean and African cultures to treat respiratory illness,

rheumatic pain, and acne (Leporatti & Ghedira, 2009). In summary, plants containing alkamides have been used as medicines by people from around the world. Many of these plants are still found in use today, although the role of alkamides in these activities has not been thoroughly defined.

1.4 Drug Interactions. There have been concerns expressed that alkamides may interact with other medications and create toxic effects. These concerns are based on reports that alkamide containing extracts from *Echinacea* interact with cytochrome P450 enzymes (M. Modarai, Gertsch, Suter, Heinrich, & Kortenkamp, 2007). Cytochrome P450 is primarily a liver enzyme and the main regulator of drug and xenobiotic metabolism (McDonnell & Dang, 2013). Initially, pure alkamides were shown to weakly inhibit various cytochrome P450 isoforms *in vitro* (M. Modarai et al., 2007). Subsequently, it was found that while enzyme activity could be suppressed to a small degree, there was no change in the levels of P450 mRNA. Since the activity of this enzyme is largely controlled transcriptionally, the authors concluded that *Echinacea* preparations were unlikely to cause interactions with additional drugs (Maryam Modarai, Silva, Suter, Heinrich, & Kortenkamp, 2010). Of additional concern is the finding that when liver microsomes are incubated with *Echinacea* alkamides, the alkamides were metabolized to a novel class of carboxylic acid and hydroxylated metabolites which were less potent immunosuppressors than unmetabolized alkamides (Nadja B. Cech et al., 2006). Cytochrome P450 enzymes may therefore limit the effectiveness of alkamides *in vivo*.

1.5 Alkamide Cellular Activities

1.5.1 Macrophages

Macrophages are critical innate immune cells involved in organ homeostasis and defense against microbes (Lavin, Mortha, Rahman, & Merad, 2015). Excess macrophage activation can, however, result in pathophysiological damage (Arango Duque & Descoteaux, 2014) and, therefore, it is necessary to identify immunomodulatory compounds which can dampen macrophage responses. Alkamides have been shown to display this activity *in vitro*. For example, alkamides have been shown to inhibit LPS-induced TNF-α production by human monocytes/macrophages (Juerg Gertsch, Schoop, Kuenzle, & Suter, 2004). The authors propose that this effect is mediated by alkamides binding to type 2 cannabinoid receptors (CB2) and altering downstream signaling via cAMP, p38/MAPK, and JNK molecules (Juerg Gertsch et al., 2004). CB2 is highly expressed on innate and adaptive immune cells, with the capability to down-regulate cellular activity, and has been proposed as an important therapeutic target (Turcotte, Blanchet, Laviolette, & Flamand, 2016). Subsequently, it was shown that the alkamides dodeca-2E,4E,8Z,10Z-tetraenoic acid isobutylamide and dodeca-2E,4E-dienoic acid isobutylamide (A15) bind the CB2 receptor directly, with a higher affinity than endogenous cannabinoids, and that binding was associated with increased intracellular calcium level and IL-6 expression. However, contradictory to previous work, it was shown that the effect on TNF-α, IL-1β, and IL-12p70 expression was independent of CB2 binding (Raduner et al., 2006). This could illustrate the presence of multiple cellular targets of alkamides resulting in inhibition of both CB2-dependent and CB2-independent pathways leading to modulation of cytokine production. Taken together, these results demonstrate that alkamides are able to directly bind an important cell surface receptor,

with known anti-inflammatory activity, as well as inhibit pro-inflammatory cytokine production through alternative, undefined mechanisms.

Alkamide effects on macrophages have also been studied during viral infection. During infection with influenza A, macrophages are key in elimination of the virus and can also contribute to the symptoms and pathology of influenza A by causing overproduction of inflammatory mediators (Cline, Beck, & Bianchini, 2017). It was found that alkamides undeca-2Z,4E-diene-8,10-diynic acid isobutylamide, dodeca-2E,4E,8Z,10E/Z-tetraenoic acid isobutylamide, dodeca-2E,4E-dienoic acid isobutylamide (A15), and undeca-2E-ene-8,10-diynoic acid isobutylamide from *Echinacea* were able to inhibit influenza-induced TNF-α and prostaglandin production, with dodeca-2E,4E-dienoic acid isobutylamide (A15) also strongly inhibiting chemokine CCL2, CCL3, and CCL5 production (N. B. Cech et al., 2010). The inhibition of these mediators may explain the relief from symptoms seen in certain individuals when *Echinacea* extracts are used to treat influenza A.

1.5.2 T cells

Thymus-derived lymphocytes, or T cells, are a type of lymphocyte whose activity is critical to the immune response to infection, allergic reactions, and cancer (B. V. Kumar, Connors, & Farber, 2018). Alkamides have been shown to inhibit IL-2 production in a dose dependent-manner from Jurkat T cells and the effects were independent of cytotoxicity (Sasagawa, Cech, Gray, Elmer, & Wenner, 2006). IL-2 production is an important signaling molecule in T cell function and differentiation and decreasing IL-2 production may limit T cell activation and proliferation reducing the adaptive immune response. On the other hand, reducing IL-2 production in certain situations may have a beneficial effect by decreasing production of pro-inflammatory cytokines

(Ross & Cantrell, 2018). In support of this hypothesis, mitogen-stimulated splenocytes harvested from mice treated with *Echinacea*, produced significantly less IL-1β and TNF-α (Zhai et al., 2007). These mice also showed enhanced levels of T cell proliferation, both mitogen-induced and in the absence of mitogens. Stimulation of T cell proliferation was also observed using a commercial preparation of *Echinacea augustifolia* in which murine T cells were stimulated with anti-CD3 and the commercial *Echinacea* product (Morazzoni et al., 2005). Finally, T cell calcium responses were also found to be inhibited follow ionophore stimulation upon treatment with dodeca-2E,4E-dienoic acid isobutylamide (A15) (T. V. Gulledge et al., 2018).

1.5.3 Mast Cells

Alkamides have been shown to be biologically active against mast cells. Mast cells are myeloid derived immune cells with key roles in regulation of vascular homeostasis, immune responses, and angiogenesis and have important functions in diseases such as allergy, asthma, cardiovascular disorders, and gastrointestinal diseases (Krystel-Whittemore, Dileepan, & Wood, 2016). Alkamide A15 was demonstrated to inhibit mast cell degranulation, histamine release, and calcium influx in both primary bone marrow mononuclear cells and the mast cell-like line RBL-2H3 (T. V. Gulledge et al., 2018). Because A15 was able to block granule release following ionophore stimulation, as well as FCεRI crosslinking, A15 must act on molecular targets regulating both stimulation pathways. Additionally, A15 inhibited TNF-α and prostaglandin E2 production following ionophore stimulation. In an atopic dermatitis model, mast cell tissue infiltration was diminished following treatment with spilanthol (Huang, Huang, Hu, Peng, & Wu, 2019). *In vivo*, oral administration of N-(2-hydroxyethyl) hexadecanamide downregulated mast cell activation and pathology associated with mast cell activation such as edema (Mazzari, Canella, Petrelli,

Marcolongo, & Leon, 1996). In an asthmatic model using OVA-sensitized guinea pigs, *Echinacea* treated animals displayed a significant reduction in exhaled nitric oxide which has been shown to be partially produced by mast cells in asthmatic disease (Šutovská et al., 2015).

1.5.4 Neurons

Another popular therapeutic use for alkamides is as pain relievers. Numerous groups have now reported on the analgesic effects of alkamides *in vitro* and *in vivo*. There are multiple types of pain receptors, with different specific receptors mediating mechanical and thermal pain. The neurons bearing these receptors are categorized as C-fibers, which are unmyelinated and small in diameter, and A-fibers, which are myelinated and quick to respond to stimuli mediating "initial fast-onset pain" (Dubin & Patapoutian, 2010). Using the alkamide hydroxy-α-sanshool, from the *Zanthoxylum* plant, a selective inhibition of mechanical pain via inhibition of voltage-gated sodium channels on Aδ mechanonociceptors was observed in mice under both naïve and inflammatory conditions, with no influence on thermal pain (Tsunozaki et al., 2013). Hydroxy-α-sanshool also altered activity levels of cool-sensitive fibers and cold nociceptors in extracellular nerve recording from the lingual nerve in rats (Bryant & Mezine, 1999). Sanshool was also found to target transient receptor potential (TRP) channels TRPV1 and TRPA1 (Menozzi-Smarrito, Riera, Munari, Le Coutre, & Robert, 2009). Alkamides from *Acmella oleracea* and a synthetic isobutylalkylamide showed long lasting *in vivo* analgesic efficacy when mice were pretreated with the alkamide 15 minutes prior to carrageenan injection to induce pain (Dallazen et al., 2020). Alkamide A15 was demonstrated to be biologically active in the central nervous system in mice following intraperitoneal injection and dependent on interaction with the voltage-gated sodium channel, particularly Nav1.8 (Gertsch 2008a). TRPV1, a non-specific cation channel that is the receptor for

capsaicin and found on neurons, has been shown to be sensitive to isobutylalkylamides (Fan Yang Jie, 2017). Using *in vitro* dorsal root ganglion cultures, neurons responded to the application of a synthetic isobutylalkylamide with an increase in intracellular calcium in a manner similar to activation by capsaicin (Tulleuda et al., 2011). This supports the analgesic effects observed with alkamides due to TRPV1 repeat activation of the channel leading to desensitization and lack of responsiveness (Jara-Oseguera 2010). Alkamides, such as pellitorine, also directly inhibit TRPV1 activation by acting as an antagonist which additionally explains the commonly observed analgesic effects (Oláh et al., 2017). This points to dual actions of alkamides as both TRPV1 agonists and antagonists, which can both lead to channel inactivation and pain relief. Interestingly, low dose synthetic isobuytlalkylamide administration was shown the be anti-nociceptive, whereas high doses induced nociceptive behaviors in mice, with the authors suggesting the anti-nociceptive effects arising from blocking of ion channels (Dallazen et al., 2018). Further, lingual application of synthetic isobutylalkylamide activated mechanosensitive neurons through modulation of potassium channels in human testing and causes a tingling sensation, repeat exposure to the isobutylalkylamide causes desensitization of the channels and lessened tingling (Albin & Simons, 2010). This supports inhibition of neuron activities through desensitization of ion channels.

1.5.5 Alkamide transport across membrane barriers

Understanding the molecular mechanisms of alkamide action is crucial for the development of alkamide-based therapies. One major hurdle in drug development is permeability of the drug across cell monolayers and membranes. Transport of alkamides across cell barriers has been studied, particularly across the gut membrane because a major traditional use of alkamide containing plants is through ingestion. Permeability across the blood brain barrier is “the single

most important factor" in drug development and permeability of alkamides may allow for a novel class of analgesics to be developed (Pardridge, 2005). The question of alkamide permeability was studied by investigating the permeability of the alkamide pellitorine using a Caco-2 cell monolayer, and two *in vivo* models evaluating the gut and blood brain barrier tissues following oral and intravenous administration, respectively. It was found that in all three instances, pellitorine was able to cross cellular barriers and be detected (Lieselotte Veryser et al., 2016). In addition to pellitorine, spilanthol was found to be highly effective at crossing the gut monolayer and entering circulation along with high blood brain barrier permeability (L. Veryser et al., 2016). while alkamides from *Echinacea* have been shown to cross a Caco-2 cell monolayer (Matthias et al., 2004). Variability in efficiency of alkamide transport across the blood-brain barrier has also been noted, and proposed as an explanation for differences in efficacy *in vivo* (Qiang et al., 2011). Although each of these studies has found alkamide transport across cellular barriers and supports the development of systemic and neurotherapeutics, none of these studies examined the mechanism of alkamide transport across cellular barriers or alkamide entry into cells.

1.5.6 Dietary and nutritional effects of alkamides

Alkamides have be tested as therapeutics for dietary and nutritional disease, particularly in diabetes. For example, daily oral administration of alkamides to diabetic rats was shown to significantly decrease fasting blood glucose level, and total liver cholesterol, and to relieve organ enlargement through activation of the AMPK signaling pathway which reduced fatty acid synthesis (Ren, Zhu, & Kan, 2017). Additionally, alkamides from *Zanthoxylum* were found to cause activation of the mTOR pathway in diabetic rats and ameliorate their protein metabolism disorder (Ren, Zhu, Xia, et al., 2017). Alkamides from the same plant also increased glucose

metabolism preventing hyperglycemia and pancreatic dysfunction through modulation of the main enzymes regulating gluconeogenesis as well as improved amino acid metabolism (Wei et al., 2020; You et al., 2015).

1.5.7 Other cellular and molecular activities

Alkamides have also been investigated as treatments for cancer. For example, alkamide derivatives of bexarotene were able to induce apoptosis and prevent cell migration and proliferation in triple-negative breast cancer cells, while showing no cytotoxic effects against normal mammary epithelial cells (Chen, Long, Nguyen, Kumar, & Lee, 2018). In addition, a panel of alkamides with varying structure and molecular weights were able to induce differentiation of human leukemia cells to granulocyte-like cells (Harpalani, Snyder, Subramanyam, Egorin, & Callery, 1993).

Alkamides have also been shown to be antimicrobial and potentially useful in farming and agricultural industry. Alkamides from *Heliopsis longipes* roots showed significant inhibition of against several fungal and bacterial species including *Saccharomyces cerevisiae*, *Escherichia coli*, and *Bacillus subtilis* (Molinatorres et al., 1996). Alkamides may also be useful as fertilizers in the agricultural industry with recent research showing that alkamides could be useful as plant growth regulators due to their ability to influence humic acid bioactivity that can improve soil properties (Y. Li et al., 2019; Zandonadi et al., 2019).

1.6. Structure & function studies

1.6.1 Fatty acid chain saturation. A number of labs have asked how the structure of various alkamides contributes to their activities. For example, the importance of double bonds in the fatty

acid chain was evaluated by measuring inhibition of cytokine production from LPS-stimulated RAW 264.7 macrophage-like cells. Similar levels of inhibition of TNF-α was observed with synthetic versions of A15 which all have 12-carbon tails with zero, one, or two double bonds indicating that unsaturated bonds are not required for inhibitory effect (Moazami, Gulledge, Laster, & Pierce, 2015). Further, 11-12 carbon isobutylamides containing a double bond at position C2 were found to inhibit chemically induced TNF-α production from human blood, RAW 264.7 macrophage-like cells, and other cell lines (Boonen et al., 2012; N. B. Cech et al., 2010).

The presence of multiple alkyne groups in the fatty acid chain was also investigated. Alkamides with multiple alkyne groups inhibited the activity COX enzymes, and at higher levels, inhibited prostaglandin E_2 production (N. B. Cech et al., 2010; Clifford, Nair, Rana, & Dewitt, 2002). Interaction with the endocannabinoid receptor CB2 has been shown to occur with unsaturated alkamides with 11-14 carbons, but there was no affinity observed for *all-trans* tetradeca-2E,4E,8E,10E-tetraenoic acid IBA, indicating specific structural requirements for alkamide receptor interaction (Boonen et al., 2012). One group showed alkamides required a double bond at the C2 position for interaction with CB2 receptors with a second double bond at C4 increasing affinity, but not required for receptor interaction (Boonen et al., 2012; Jürg Gertsch, 2008). Finally, a possible role for double bonds came from studies of the endocannabinoids where it was noted that the alkamide N-benzyl-(9Z,12Z)-octadecadienamide double bonds closely mimic those in endocannabinoid substrates (Hajdu et al., 2014).

The number and placement of double bonds has also been shown to impact the ability of alkamides to cross cell barriers. Using a Caco-2 cell monolayer, spilanthol and pellitorine, both 10 carbon alkamides but variable in position and number of double bonds, were tested for their ability to cross the monolayer. Spilanthol transport was significantly better than was the transport of

pellitorine, suggesting that the placement and number of double bonds can affect transport (Veryser 2014). A systematic analysis of bond number and position, and how they affect transport has not been performed.

Positioning of double bonds in spilanthol analogs between carbons two and five altered the physiological activity, with most activity resulting from double bonds at positions two and four (Ley, Krammer, Looft, Reinders, & Bertram, 2006). The necessity of double bonds in the fatty acid chain was also evaluated for the activity of α-hydroxysanshool. Unsaturations were found to be required for interaction with TRPA1, but not TRPV1, perhaps indicating that different regions of the alkamide interact with the two receptors (Menozzi-Smarrito et al., 2009).

1.6.2 Fatty acid chain length. The length of the fatty acid chain was investigated using synthetic variants of A15 in an LPS activated RAW 264.7 cell model system. Alkamides with fatty acid tails shorter than 12 carbons did not significantly inhibit LPS-stimulated TNF-α cytokine production, indicating that longer fatty acid chains are required for this activity (Moazami et al., 2015).

Alkamide fatty acid chain length was also evaluated in mast cells with alkamide analogs of varying chain lengths tested for their ability to inhibit intracellular calcium influx and mast cell degranulation. It was found that the shortest (four carbon) and longest (15 carbon) analogs were poor inhibitors of both degranulation and intracellular calcium influx (Collette 2017). Interestingly, there seemed to be differences in the optimum chain length and maximum inhibition for calcium influx and degranulation, perhaps suggesting different cellular targets responsible for inhibitory effects. For degranulation, the optimum chain length was eight carbons and for inhibition of calcium influx it was 12 carbons.

1.6.3. Head group. The head group was also investigated using LPS-stimulated RAW 264.7 cells and results indicated that head group substitutions were well tolerated with biological activity retained with most substitutions (Moazami et al., 2015). Addition of a carbon into the isobutyl head group did not significantly affect cytokine inhibition, and replacement of the isobutyl group with a benzyl group or six-carbon alkyl chain lessened inhibition, but the molecule was still biologically active (Moazami et al., 2015). Finally, altering of the amide functional group through addition of a thiazole group rendered the molecule inactive, thus demonstrating the importance of the amide (Moazami et al., 2015). In other studies using alkamides with benzyl headgroups, some showed affinity for CB2 receptors, which had been previous reported for isobutyl headgroups, with most activity seeming to come from the presence of an alkyl chain with 2 double bonds, rather than the identity of the headgroup (Boonen et al., 2012).

1.7 Summary

Significant progress has been made into understanding alkamide activity and use as a therapeutic, although many questions regarding the molecular mechanism of alkamide action remain unanswered. At a cellular level, only a few specific molecular targets of alkamides have been defined. It is also unclear if targets for alkamide activity are all proteins, and if those proteins share common motifs and locations on or in cells. *In vivo*, the metabolism and movement of alkamides has not been fully defined nor has it been determined whether the activities of alkamides observed during their traditional use arise from effects on specific cells, organs, and tissues. In this report we focus on a major unresolved question regarding alkamide activity-- do alkamides gain entry into cells? To address this question, we have used confocal microscopy to study the association of a novel fluorescein-tagged alkamide with RAW 264.7 macrophage-like cells. Our

experiments reveal that this alkamide does indeed enter cells, through a form of clathrin-dependent endocytosis and likely localizes within $Rab7^{+}$ late-stage endosomes. We believe, therefore, that the constellation of targets for alkamide activity grows dramatically as does their possible mechanisms of action.

CHAPTER 2: METHODS

2.1 Reagents

Lipopolysaccharide (Salmonella Minnesota R595) was purchased from List Biological Laboratories, Campbell, CA, USA. Texas Red-dextran 3000 MW (cat. D3328), cytochalasin D, and ProLong Gold Antifade Mountant were purchased from Thermo Fisher Scientific, Waltham, MA, USA. Tumor necrosis factor enzyme-linked immunosorbent assay was purchased from eBioscience, San Diego, CA, USA, and 4% paraformaldehyde in phosphate buffered saline was purchased from Affymetrix, Cleveland, OH, USA. Triton X-100 was purchased from Sigma-Aldrich, St. Louis, MO, USA. The endosomal marker antibody kit was purchased from Cell Signaling Technology (cat. No. 12666) from Danvers, MA, USA. Deuterated solvents (containing 0.03 to 0.05 vol % tetramethylsilane, TMS) were purchased from Cambridge Isotope Laboratories, Tewksbury, MA, USA. All other reagents were purchased from commercial chemical companies and used without further purification, unless otherwise stated.

2.2 Cell culture

All cell lines (RAW 264.7, Vero, and RBL-2H3) were purchased from the American Type Culture Collection (Manassas, VA, USA). Fetal bovine serum was purchased from Gemini BioProducts, West Sacromento, CA, USA, with non-essential amino acids from GE Life Sciences, Marlborough, MA, USA, and sodium pyruvate was purchased from Mediatech, Inc., Manassas, VA, USA. All other cell culture reagents and plasticware were purchased from Genesee Scientific, Raleigh, NC. Murine RAW 264.7 macrophage-like cells were cultured in Dulbecco's Modified Eagle's Medium (DMEM) containing 4mM L-glutamine, 4.5g/L glucose, and 1.5g/L sodium pyruvate and supplemented with 10% fetal bovine serum at 37°C and 5% CO_2. Vero cells were

grown in Minimum Essential Medium Eagle with Earle's salts and 4mM L-glutamine, supplemented with 6% fetal bovine serum at 37°C and 5% CO_2. RBL-2H3 cells were grown in Minimum Essential Medium Eagle with 2mM L-glutamine, 1.5gL/ sodium bicarbonate, 1mM non-essential amino acids, 1mM sodium pyruvate, and 15% heat-inactivated fetal bovine serum at 37°C and 5% CO_2.

2.3 Synthesis and analysis of the FITC-alkamide (performed in the lab of Dr. Joshua Pierce by You-Chen Lin)

2.3.1 Synthesis of FITC-Alk

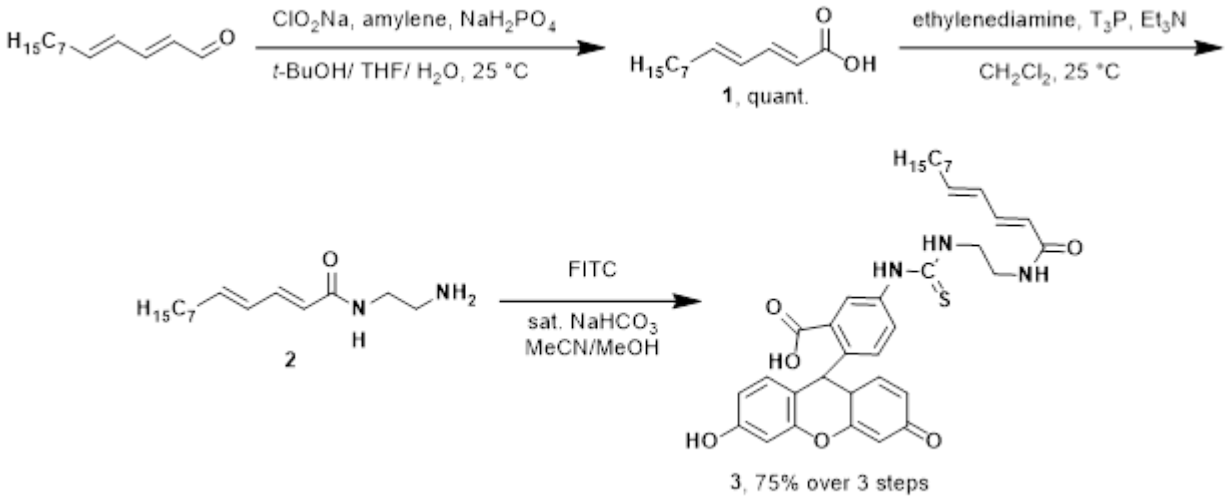

Figure 2.1. Overview of the synthesis of FITC-Alk. To make the FITC-Alk molecule, (2E,4E)-dodeca-2,4-dienal was used as a starting compound and crud fatty acid 1 was produced. Then crude fatty acid 2 was synthesized to which a fluorescein (FITC) molecule was substituted for the headgroup to generate the FITC-Alk molecule.

(2E,4E)-Dodeca-2,4-dienoic acid (1): To a solution of the (2E,4E)-dodeca-2,4-dienal (0.3 g, 1.50 mmol, 1.0 equiv) and amylene (1.05 g, 14.98 mmol, 10.0 equiv) in t-BuOH/THF 1:1 (6 mL) at 0 °C was added a solution of sodium chlorite (0.34 g, 3.00 mmol, 2.0 equiv) and sodium dihydrogen phosphate (0.36 g, 3.00 mmol, 2.0 equiv) in water (2 mL). The reaction was allowed to warm to 25°C. After 20 h, the mixture was poured into water (10 mL) and diluted with EtOAc (3 mL). The aqueous layer was extracted with EtOAc (3 x 10 mL) and the organic layers were combined, dried (Na2SO4) and concentrated under reduced pressure to afford quantitative crude fatty acid 1, which was used in the subsequent step without further purification.

5-(3-(2-((2E,4E)-Dodeca-2,4-dienamido)ethyl)thioureido)-2-(6-hydroxy-3-oxo-9,9a-dihydro-3H-xanthen-9-yl)benzoic acid (3): To a solution of crude fatty acid 1 (0.196 g, 1.00 mmol, 1.0 equiv) in CH2Cl2 (10 mL) was added Et_3N (0.404 g, 4.00 mmol, 4.0 equiv) and T3P® (0.762 g, 1.20 mmol, 1.2 equiv) at 25°C. After 15 min, ethylenediamine (0.067 g, 1.10 mmol, 1.1 equiv) was added and the mixture was stirred for 3 h then filtered off the solid, the filtrate was evaporated under reduced pressure. The crude residue was dissolved in EtOAc (10 mL), and the organic layer was washed with brine (5 mL) and water (5 mL), dried (Na_2SO^4) and concentrated under reduced pressure to afford crude amide 2, which was used in the subsequent step without further purification.

The crude amide 2 (34.2 mg, 0.14 mmol, 6.2 equiv) residue was dissolved in sat. aq. NaHCO3/MeCN/MeOH 2.5:1:1 (4.5 mL) at 25 °C and was added fluorescein isothiocyanate (10.0 mg, 0.23 mmol, 1.0 equiv) in the absence of light. After 5 h, the reaction was quenched (sat. aq. NH^4Cl, 5 mL), the aqueous layer was extracted with EtOAc (3 x 10 mL) and the organic layers were combined, dried (Na_2SO^4) and concentrated under reduced pressure. The crude residue was

purified by column chromatography (SiO2, gradient elution: 0% to 18% MeOH in CH_2Cl^2) to afford the FITC-alkamide 3 (10.9 mg, 75% over three steps).

2.3.2 Synthesis of FITC-A-12, FITC-A-8, and FITC-A-4

Synthesis of FITC-A-12, FITC-A-8, and FITC-A-4 was carried out in a similar manner to that described above in the synthesis of FITC-Alk. The overview of the synthesis of FITC-A-12 and FITC-A-8 molecules is outlined in **Figure 2.2 A**, and the overview of the synthesis of FITC-A-4 is outlined in **Figure 2.2 B**.

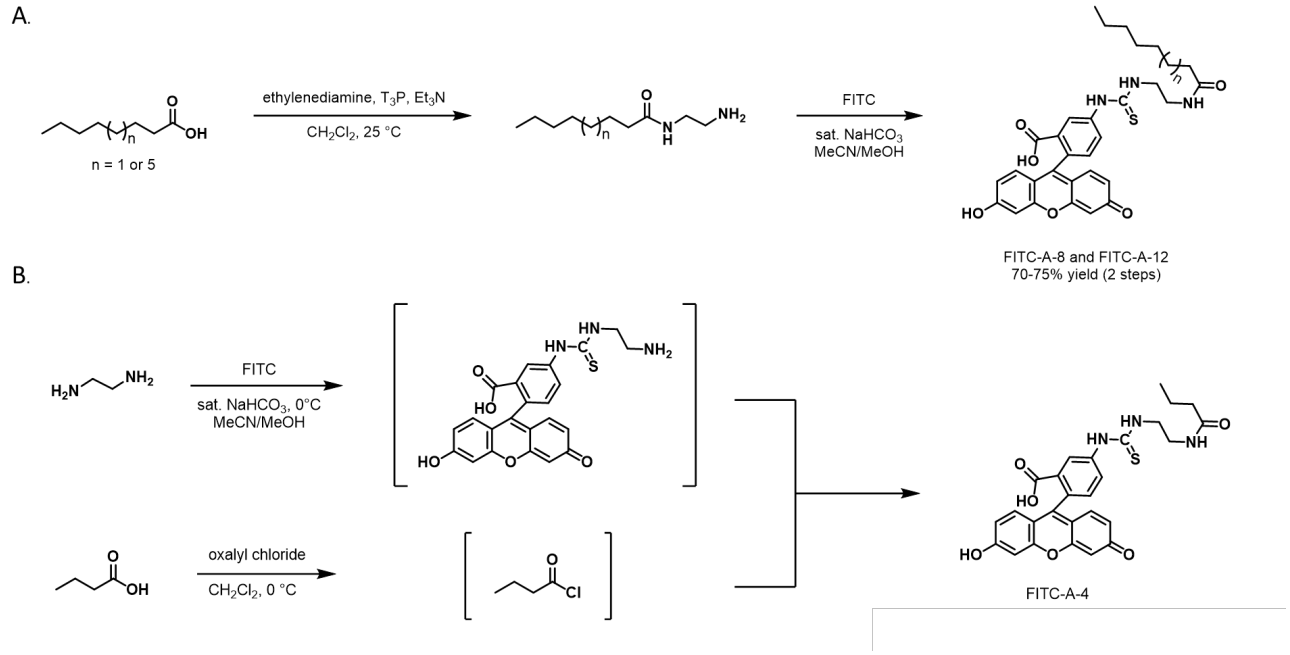

Figure 2.2. Overview of the synthesis of FITC-Alk-12, FITC-A-8, and FITC-A-4. (A) FITC-A-12 and FITC-A-8 were synthesized by obtaining the desired alkamide structure from a carboxylic acid precursor and attaching the FITC molecule to the headgroup. (B) FITC-A-4 was synthesized by adding the FITC molecule to an amine molecule and reacting with an acid chloride molecule.

2.4 Confocal microscopy

RAW 264.7 cells were plated in 8-well Nunc Lab-Tek II Chamber Slides (Thermo Fisher Scientific, Waltham, MA, USA) at a density of $5x10^4$ cells per well. RBL-2H3 mast cell-like cell line and Vero kidney epithelial cells were seeded at a density of 7.5×10^4 cells per well. For most experiments, unless otherwise stated, cells were stained with FITC-Alk for 15 min, washed 3 times with sterile phosphate buffered saline solution (PBS), fixed with cold 4% paraformaldehyde in PBS for 10 minutes at room temperature, and washed 3 times with sterile PBS. The slides were then mounted with a #1.5 thickness coverslip, sealed with clear nail polish, and shielded from light until visualization.

For methanol fixed cells, seeded cells were fixed with chilled 100% methanol for 5 minutes at room temperature, washed 3 times with sterile PBS, stained and mounted as described above. Cells fixed prior to staining with paraformaldehyde were fixed with 4% paraformaldehyde in PBS for 10 minutes at room temperature, washed 3 times with sterile PBS, stained with FITC-Alk, washed again 3 times with sterile PBS, then mounted as described above.

Endoplasmic reticulum staining cells were seeded and fixed with 4% paraformaldehyde for 10 minutes at room temperature. Cells were then washed 3 times with sterile PBS and permeablized with 0.1% Triton X-100 (Sigma-Aldrich, St. Louis, MO, USA) for 30 minutes. Cells were washed 3 times with sterile PBS and stained with 0.1mg/mL Concanavalin A, Alexa Fluor 594 Conjugate (Thermo Fisher Scientific, Waltham, MA, USA) diluted in 0.1M sodium bicarbonate (pH 8.3) buffer for 45 minutes. Cells were then washed 3 times with sterile PBS and mounted as described above.

Cytochalasin D (CytD) experiments were conducted by treating RAW 264.7 cells with 2μM CytD for 1 hr at 37°C and 5% CO^2. Cells were then stained with FITC-Alk and fixed and

stained with 1 μg/mL rhodamine-phalloidin in 4% paraformaldehyde in PBS for 10 min at room temperature. Cells were then washed, mounted, and visualized.

For double labeling with FITC-Alk and Texas Red-dextran, RAW 264.7 cells were plated as described above. Twenty-four hours post plating, cells were treated with 40 μM FITC-Alk and 40 μM or 400 μM Texas Red-dextran 3000 MW in DMEM for 15 min at 37°C and 5% CO_2. Cells were washed, fixed with 4% paraformaldehyde, mounted, and imaged as described above.

Endosome inhibition assays were conducted by pre-treating cells with 450mM sucrose (Sigma-Aldrich, St. Louis, MO, USA) or Pitstop 2 (Sigma-Aldrich, St. Louis, MO, USA) for 15 minutes. Cells were then washed and stained with FITC-Alk or Texas Red-dextran for 15 minutes and mounted as described above.

For experiments with endosomal pathway antibodies, cells were plated, washed, and fixed in paraformaldehyde as above. Cells were then permeabilized using PBS containing 0.1% Triton X-100 and blocked with 1% BSA, 22.25 mg/mL glycine in PBST. Primary antibodies were added in 1% BSA PBST overnight at 4 oC at the following dilutions; caveolin-1 (1:400), clathrin heavy chain (1:50), early endosome antigen-1 (1:100), Rab7 (1:100), and Rab11 (1:100). Cells were washed and Alexa Fluor-488 labeled goat α-rabbit IgG (Molecular Probes, Eugene, OR, USA) secondary antibody was added for 1 hour at room temperature in the dark, washed and mounted as described above.

Cells were visualized using a C-Apochromat 40x water immersion objective lens on a Zeiss LSM 880 confocal microscope using 405 nm, 488 nm, and 561 nm excitation lasers. Light was collected at the 411-484 nm (DAPI), 490-552 nm (FITC/AlexaFluor 488), and 560-678 (Texas Red/rhodamine phalloidin/AlexaFluor 594) range depending on the experiment.

Corrected total cell fluorescence (CTCF) was measured in three biological replicates only in the experimental channel (e.g. FITC channel) in ImageJ. CTCF was calculated from the following formula (integrated density – (area * mean fluorescence of the background)). Ten cells were selected, calculating the integrated data via ImageJ and then calculating the mean background fluorescence from 10 random background readings. The area of the cell was multiplied by the mean fluorescence of the background readings, and the product was subtracted from the product of the area and the mean grey value (integrated density) of each cell which were then averaged together for each biological replicate. Results are presented as a mean of 3 (n=3) biological replicates ± SEM.

2.5 Alkamide structure:function endocytosis assay

Alkamide structure function endocytosis assay was done by plating 1 x 10^5 RAW 264.7 cells in black, clear bottom 96-well plates (Genesee, San Diego, CA, USA). Cells were treated with 50 μM FITC-Alk, FITC-Alk-12, FITC-Alk-8, or FITC-Alk-4 for 15 minutes at 37°C and 5% CO_2. Cells were then washed three times with sterile PBS and fluorescence was measured using a Synergy 2 HT microplate reader with 485/20 nm excitation and 528/20 nm emission filters (BioTek Instruments, Inc, Winooski, VT). Results are presented as a mean of 3 (n=3) biological replicates ± SEM.

2.6 Statistical analysis

Statistical analysis was performed using GraphPad Prism 5 (GraphPad, San Diego, CA, USA). Statistical significance was calculated using a one-way ANOVA with Tukey posttest with a 95% confidence interval with $p<0.05$.

CHAPTER 3: RESULTS

3.1 Synthesis of the FITC-Alk and biological activity (synthesis performed in the lab of Dr. Joshua Pierce by You-Chen Lin and biological activity was tested by Dr. Travis Gulledge)

As the first step in these experiments, a fluorescent alkamide analog was produced by replacing the head group of the naturally occurring alkamide from *Echinacea purpurea* (2E,4E)-N- isobutyldodeca-2,4-dienamide with fluorescein isothiocyanate (FITC) (**Figure 3.1 A**) since Moazami et al. (Moazami et al., 2015) showed that the isobutyl head group was not critical for the anti-inflammatory activity of this alkamide. We evaluated the biological activity of this FITC labeled alkamide (FITC-Alk) molecule by testing its ability to inhibit production of TNF-α from LPS activated macrophages compared to the unlabeled alkamide. We found that at concentrations of 50 and 100 μM, FITC-Alk retained biological activity comparable to the control (**Figure 3.1 B**). In contrast we did not find significant inhibition of TNF-α production with FITC itself (**Figure 3.1 B**).

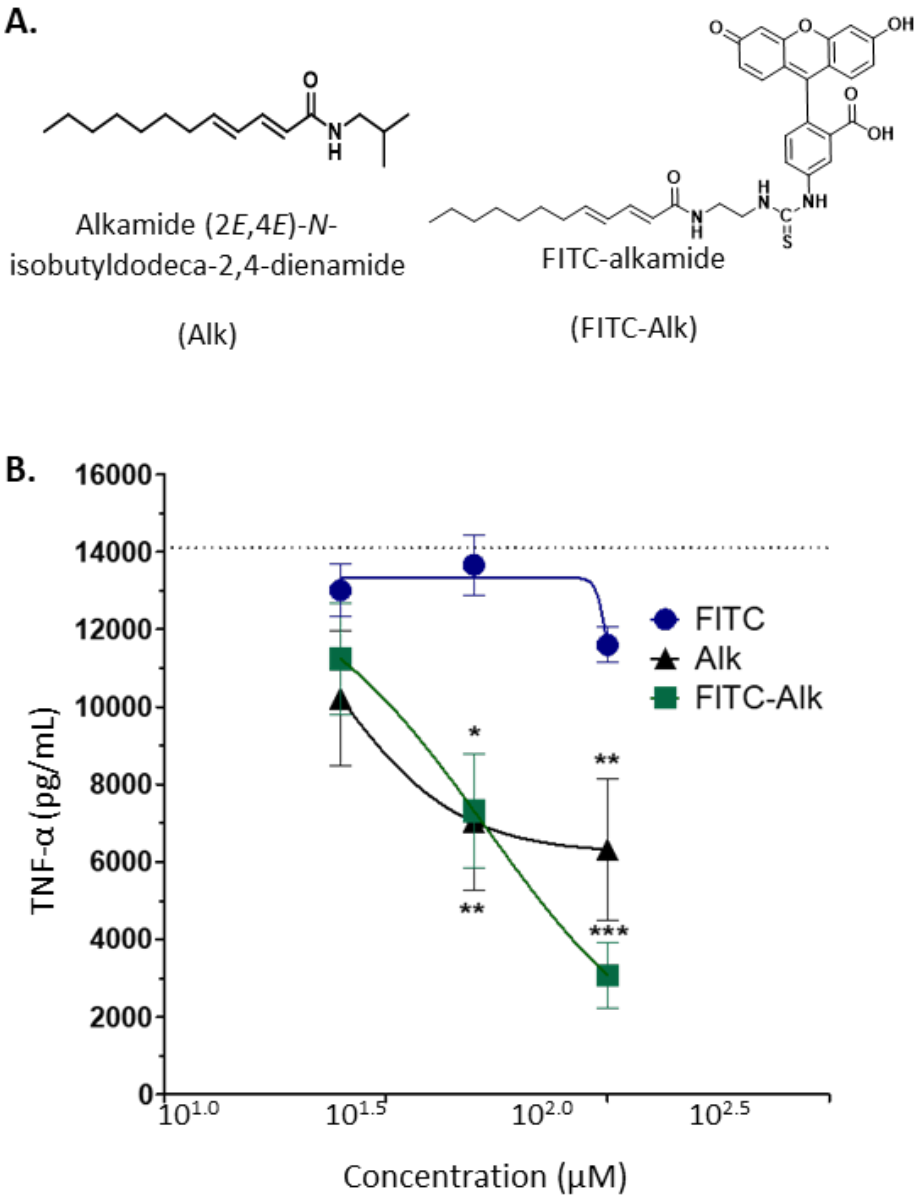

Figure 3.1. The structure and biological activity of FITC-Alk. Structures of the alkamide (2E,4E)-N-isobutyldodeca-2,4-dienamide (Alk) and the fluorescent alkamide analog (FITC-Alk) where the isobutyl group has been replaced with fluorescein (FITC) (A). RAW 264.7 macrophage-like cells were activated with 1 μM LPS overnight in the presence of alkamide, FITC-alk, or FITC alone. Twenty-four hours later, TNF-α production was measured by ELISA in three independent trials (B).

3.2 Effects of fixation reagent and processing on alkamide staining

In order to study the uptake of FITC-Alk using confocal microscopy we first sought to optimize our fixation procedure. A series of experiments were performed with different fixatives as well as varying the order of fixation and staining. When live RAW 264.7 cells were stained with FITC-Alk and then fixed with 4% paraformaldehyde large bright puncta and smaller diffuse pinpoint staining was observed (**Figure 3.2 A**). This pattern strongly resembled the pattern seen with live cell staining although the fluorescence faded extremely rapidly (data not shown) which did not allow us to produce a publishable image and thus necessitating the need for a fixation step. In contrast, fixing cells with 4% paraformaldehyde prior to staining with FITC-Alk resulted in a loss of the large bright puncta with diffuse staining throughout the cell including the nucleus (**Figure 3.2 B**). We concluded from these studies that paraformaldehyde fixation after FITC-Alk treatment likely preserved the normal biological process responsible for alkamide uptake, while fixation prior to staining, inactivated this process and produced artifactual results. We also tested methanol as a fixative prior to staining which is known to dehydrate cells and solubilize their lipid constituent (Hobro & Smith, 2017). With methanol, a bright non-specific stain pattern was observed throughout the cell suggesting, again not resembling the pattern seen with live cells, and suggesting that lipids play a role in the staining pattern observed with paraformaldehyde fixation subsequent to FITC-Alk treatment (**Figure 3.2 C**). Similarly, we found that detergent permeabilization prior to fixation also altered the staining pattern shown in **Figure 3.2 A.** When cells were stained, fixed with 4% paraformaldehyde, then permeabilized with 0.1% Triton X-100 in PBS there was a total loss of FITC-alkylamide staining (**Figure 3.2 D**). Triton, like methanol, also disrupts lipids in cells, further indicating a role for lipid integrity in puncta formation (Faulk & Badylak, 2014). Because we were unable to use detergent permeabilization and preserve

staining with FITC-Alk, we were unable to perform co-staining experiments with antibodies where membrane permeabilization is required.

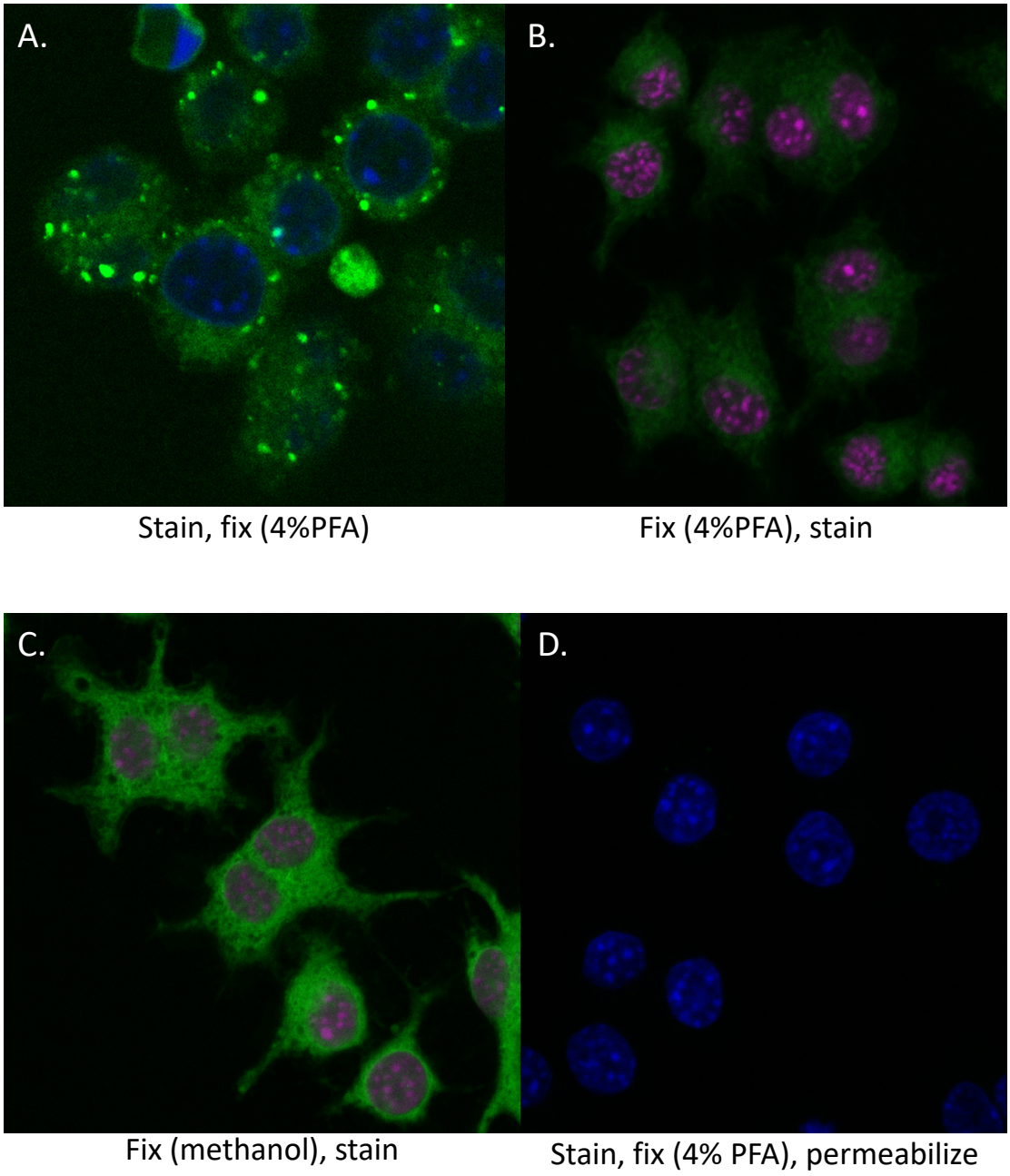

Figure 3.2. The effects of different fixatives and order of fixation on FITC-Alk staining. RAW 264.7 cells were stained live with FITC-Alk and fixed with 4% paraformaldehyde (A). Cells were fixed with paraformaldehyde (B) or methanol (C) prior to staining with FITC-Alk. Cells were stained with FITC-Alk, fixed with paraformaldehyde, and permeabilized with 0.1% Triton X-100 in PBS.

3.3 FITC-Alk enters cells in a time- and concentration-dependent manner

Having established a useful fixation and staining protocol, we next began to characterize the uptake of FITC-Alk by RAW 264.7 cells. As shown in **Figure 3.3 A-E**, we found that when 100μM FITC-Alk was added to RAW 264.7 cells in culture, increasing intracellular fluorescence was noted at 15, 30, 60, and 240 minutes. The intracellular stain pattern was composed of large bright puncta with smaller, pinpoint staining, both occurring in the cytoplasmic compartment (**Figure 3.3 A-D**). FITC itself did not produce detectable staining (**insert in Figure 3.3 A**). Quantitatively, using corrected total cell fluorescence (CTCF), there was significantly more intracellular staining after 240 min compared to 15 min ($p=0.023$, one way ANOVA with Tukey post-test), with means of 233,747±16,725 and 145,161±22,298 CTCF respectively (n=3) (**Figure 3.3 E**).

We also found that the uptake of FITC-Alk was concentration dependent (**Figure 3.4**). Staining with 1 and 10 μM FITC-Alk resulted in dim fluorescence with 1 μM producing staining barely detectable. Higher concentrations (50 and 100 μM) resulted in bright images with higher CTCF values. The mean CTCF values were 15,297 ± 3,602, 35,844 ± 4,612, 93,247 ± 3,587, and 137,134 ± 21,535 at 1, 10, 50, and 100 μM, respectively (n=3) (**Figure 3.4)**. There was a significant increase in CTCF seen between most treatment groups ($p<0.05$).

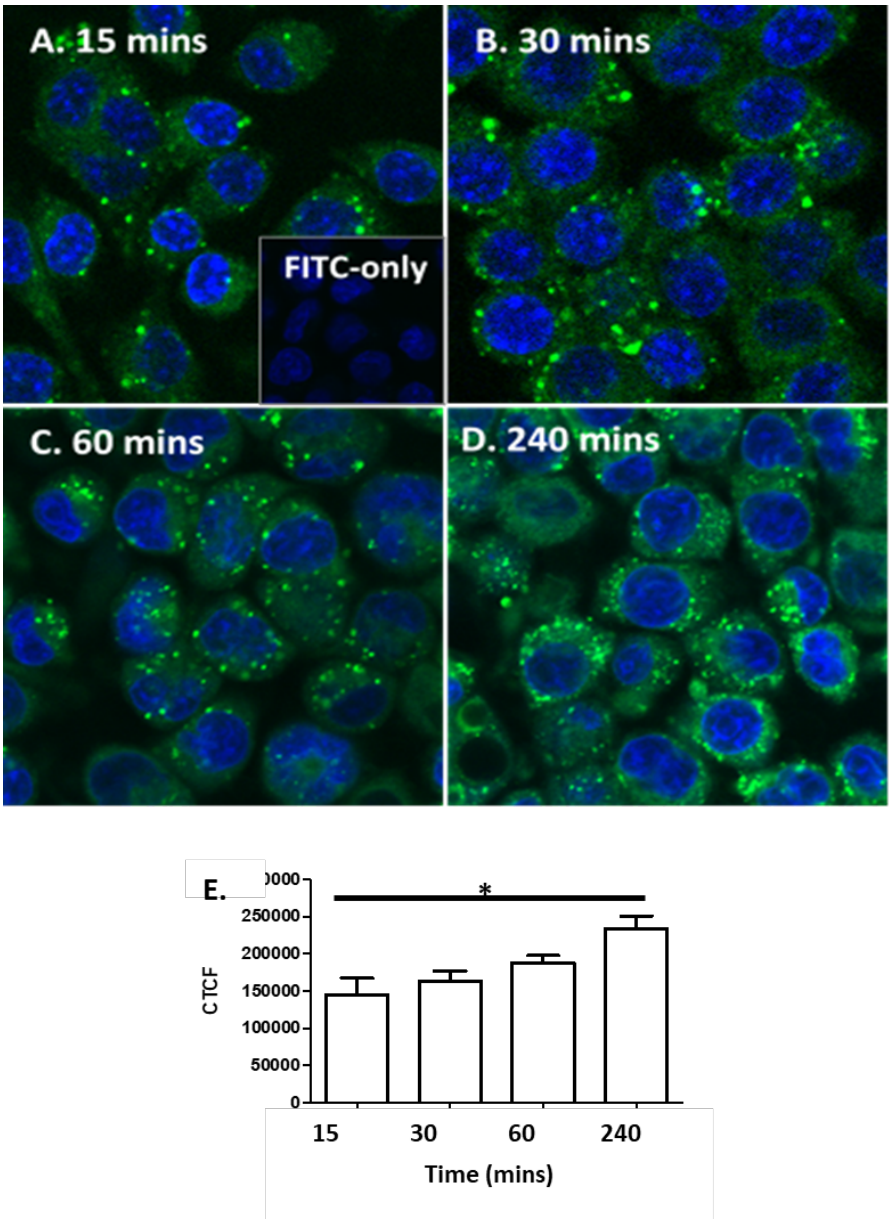

Figure 3.3. FITC-Alk is taken into RAW 264.7 cells in a time-dependent manner. Representative images showing that staining intensity increases in a time-dependent manner in RAW 264.7 macrophage-like cells stained with FITC-Alk for 15 (A), 30 (B), 60 (C), or 240 min (D) prior to fixation. DAPI was included in the mounting media to identify nuclei. Staining with only FITC is shown in the inset in A and did not reveal a visible signal. Quantitative analysis showing differences in corrected total cell fluorescence (CTCF) between time points (n=3) ± SEM (E). Significance was determined using a one-way ANOVA with Tukey posttest, $p = 0.023$.

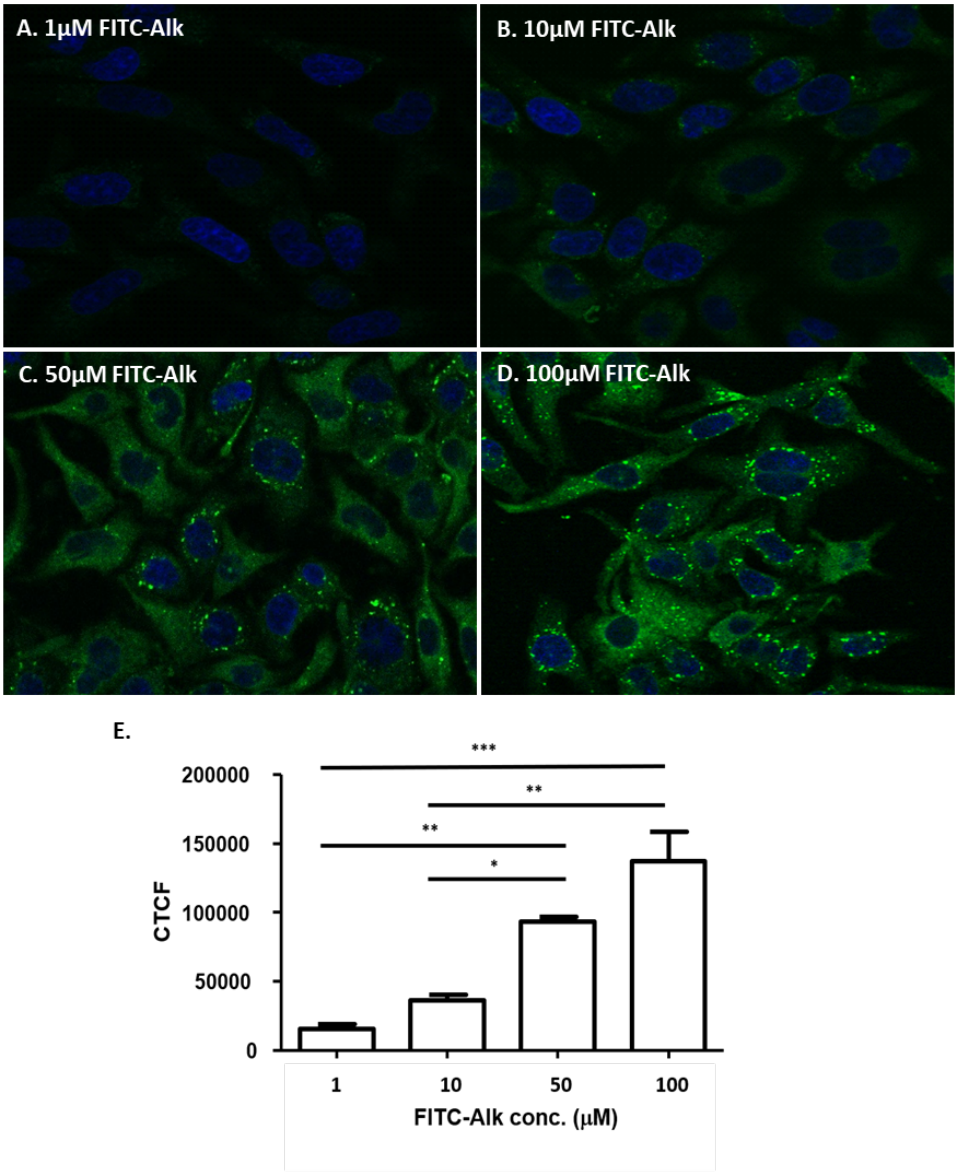

Figure 3.4. Staining with FITC-Alk is concentration dependent. Representative images showing staining intensity increases in a concentration-dependent manner. RAW 264.7 macrophage-like cells were treated with 1 (A), 10 (B), 50 (C), or 100 µM (D) FITC-Alk for 15 min prior then washed and fixed with paraformaldehyde. DAPI was included in the mounting media to identify nuclei. Quantitative analysis showing differences in correct total cell fluorescence (CTCF) between concentrations ± SEM (n=3) measured by one-way ANOVA with Tukey's posttest (E). *p<0.05, **p<0.01, ***p<0.005

3.4 Three-dimensional (3D) reconstruction of FITC-Alk staining in RAW 264.7 cells.

The intracellular distribution of the large puncta produced by FITC-Alk staining was evaluated via laser scanning confocal microscopy using an 18 μm Z-stack reconstructed to produce a 3D image using the Zeiss Zen software. Upon 3D reconstruction, we found that the bright puncta were located throughout the cell body, but more commonly found in the perinuclear region, as compared to the periphery of the cell (**Figure 3.5**). Using the same 3D reconstruction, we assessed the orientation of the puncta within the cell via depth coding where puncta very close to the coverslip (0-2 Åμm) appear red to orange, those at mid-depth (4-12 Åμm) mostly green, and those closer to the slide (14-16 Åμm) appear blue (**Figure 3.5**). The puncta were found at varying depths within many cells as indicated by puncta in all colors corresponding to all depth.

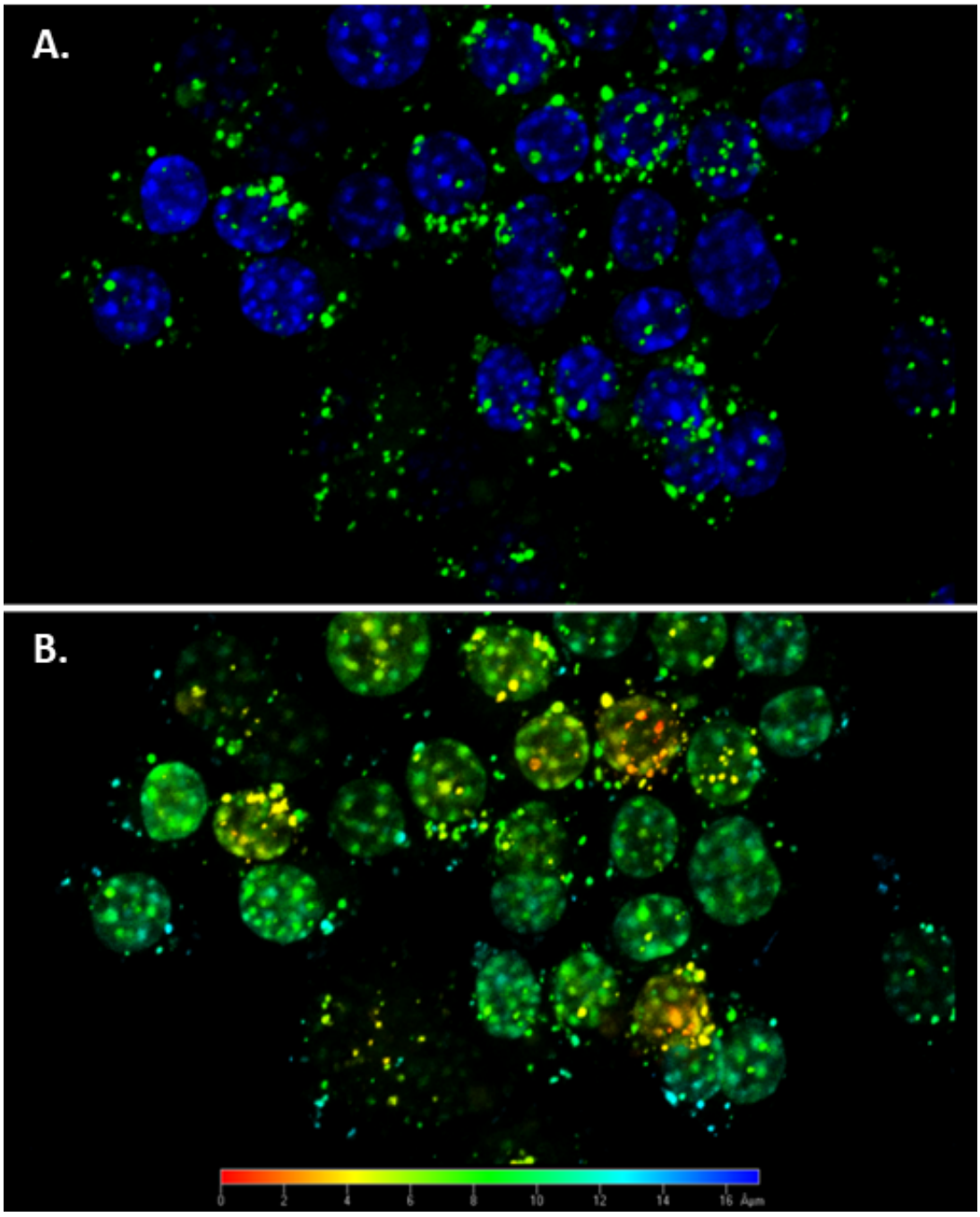

Figure 3.5. FITC-Alk puncta are found in a non-polarized orientation. 3-dimensional (3D) reconstruction of 18 μm z-stack of RAW 264.7 cells stained with 50 μM FITC-Alk for 15 min. 3D depth coding made from z-stack reconstruction showing depth map and positioning of puncta within the cells, ranging from the closest to the coverslip (0-2 Åμm) to those closest to the slide (14-16 Åμm). 3D rendering was done using Zeiss Zen software.

3.5 The pattern of staining with FITC-Alk is similar among different cell types.

To determine if the pattern of staining noted with RAW 264.7 cells is unique to this cell type, experiments were also performed with Vero green monkey kidney cells and RBL-2H3 basophilic carcinoma cells. The cells were incubated with 50μM FITC-Alk for 15 min, fixed, and observed by confocal microscopy. Overall, we noted that the resulting stain pattern was very similar among all cell types tested (**Figure 3.6 A-C**). As before, the staining pattern consisted of diffuse, pinpoint staining with large bright puncta found especially in the perinuclear region (**Figure 3.6 A-C**).

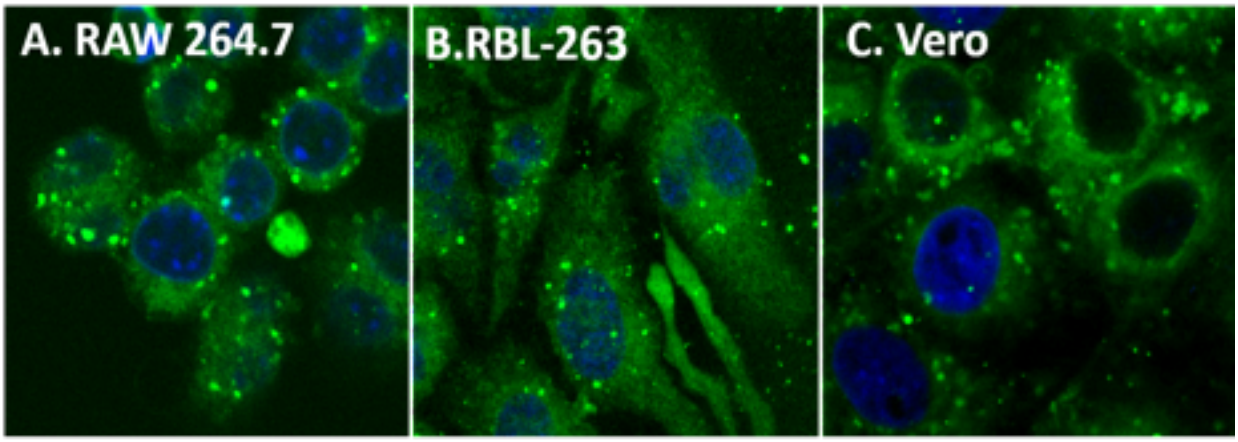

Figure 3.6. The FITC-Alk stains a variety of cell types. FITC-Alk staining of several cell types including RAW 264.7 macrophage-like cells (A), RBL-2H3 basophilic leukemia cells (B), and Vero kidney epithelial cells (C). Cells were stained with 50 μM FITC-Alk for 15 min prior to fixation. DAPI was added with the mounting media to identify nuclei.

3.6 FITC-Alk does not stain endoplasmic reticulum or mitochondria

Next, we sought to identify the intracellular compartment that may account for the bright puncta seen in FITC-Alk stained cells. AlexaFluor594-concanavalin A was used to visualize the

endoplasmic reticulum (**Figure 3.7 B**). Concanavalin A is a lectin from the jack bean and binds to the endoplasmic reticulum (Reeke et al., 1975; Schneider & Sievers, 1981). The resulting stain pattern did not match that seen with FITC-Alk lacking the bright puncta with a more diffuse staining pattern throughout the cell (**Figure 3.7 A and B**). Next, mitochondria were stained using Rhodamine 123, which is a dye that binds to negatively charged mitochondria membranes (Chazotte 2010). Again, the resulting stain pattern did not match the FITC-Alk stain pattern (**Figure 3.7 A and C**). The mitochondrial stain lacked discrete bright puncta, with most staining seen in perinuclear region.

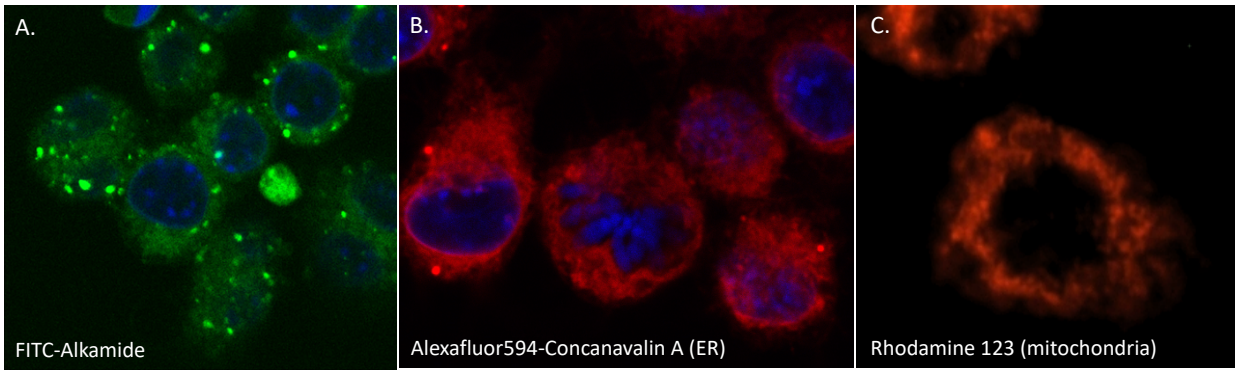

Figure 3.7. FITC-Alk staining compared to intracellular compartment stains. RAW 264.7 cells were stained with FITC-Alk (A) and compared to cells stained for endoplasmic reticulum (B) and mitochondria (C). Nuclei were visualized using DAPI.

3.7 FITC-Alk enters cells through endocytosis.

The rapid appearance of the large bright puncta in all the cells types we examined led us to ask whether the FITC-Alk molecule was accumulating in an endosomal compartment. To answer this question, we performed a double labeling experiment with equal amounts of the FITC-Alk and Texas Red-labeled dextran, a well-established endosome marker (L. Li et al., 2015). We found

that FITC-Alk and Texas Red-dextran colocalized in the same bright puncta, resulting in a yellow color (**Figure 3.8 A-C**). Additional evidence for FITC-Alk endosome accumulation was found in a competition experiment where the Texas Red-dextran was used at a concentration 10-fold higher than the FITC-Alk. As shown in **Figure 3.8 D-F**, 400 μM Texas Red-dextran reduced the formation of large puncta by 40 μM FITC-Alk.

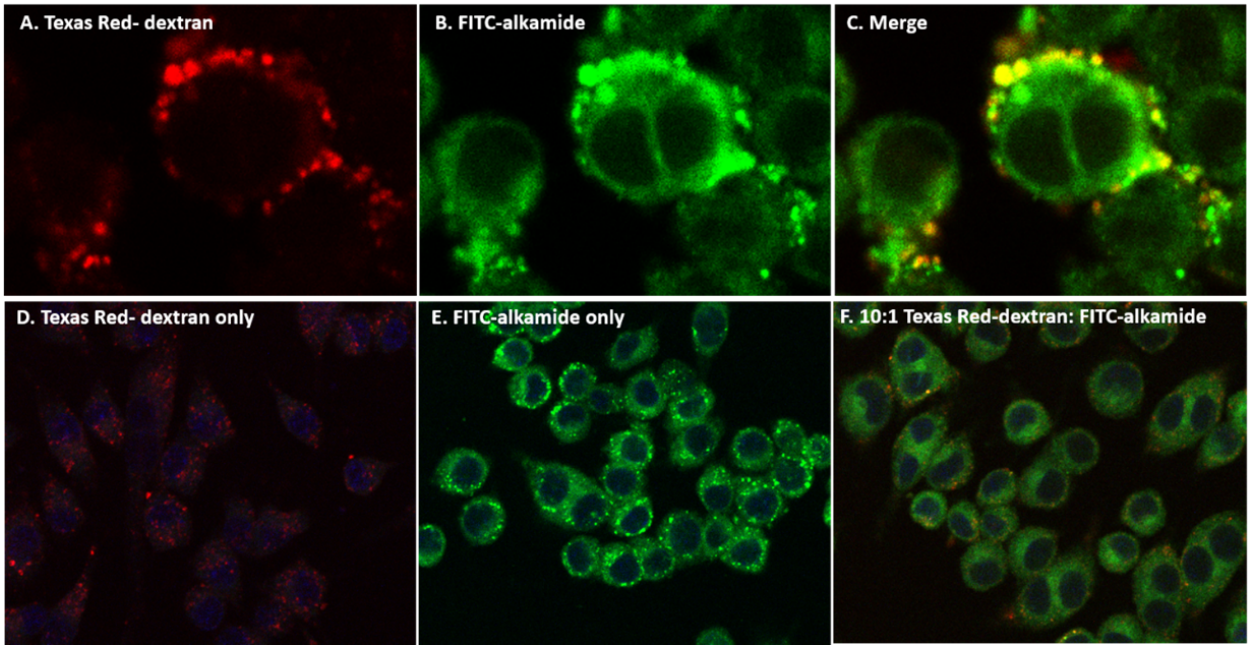

Figure 3.8. Double staining with FITC-Alk and Texas Red-dextran. Representative images showing double staining of RAW 264.7 macrophage-like cells with 1:1 mixture of 40 μM Texas Red-dextran and 40 μM FITC-Alk for 15 min (A-C). Competition experiment with 400 μM Texas Red-dextran and 40 μM FITC-Alk (D-F). Cells were stained for 15 min prior to fixation.

3.8 Alkamide puncta formation is blocked upon inhibition of clathrin-dependent endocytosis.

There are many forms of endocytosis including clathrin-dependent and -independent pathways. To investigate the mechanism of endocytic entry used by the FITC-alkamide compound

we inhibited different endocytic pathways. RAW 264.7 cells were treated with either Pitstop 2, a clathrin-independent and clathrin-dependent endocytosis inhibitor, or hypertonic sucrose, which inhibits clathrin-mediated endocytosis (**Figure 3.9)** (Dutta & Donaldson, 2012; Heuser & Anderson, 1989). Texas Red-dextran was used as a positive control for endocytosis inhibition. We found that treatment with hypertonic sucrose, but not Pitstop 2, lessened FITC-Alk puncta formation indicating a role for the clathrin-mediated endocytic pathways in puncta formation. Additionally, cells were relatively dimmer in the hypertonic sucrose treatment groups compared to untreated and Pitstop 2 treated cells. Pitstop 2 did not affect FITC-Alk puncta formation or overall staining intensity. Therefore, the clathrin-mediated pathway is most likely the primary mechanism of alkamide entry leading to large puncta formation

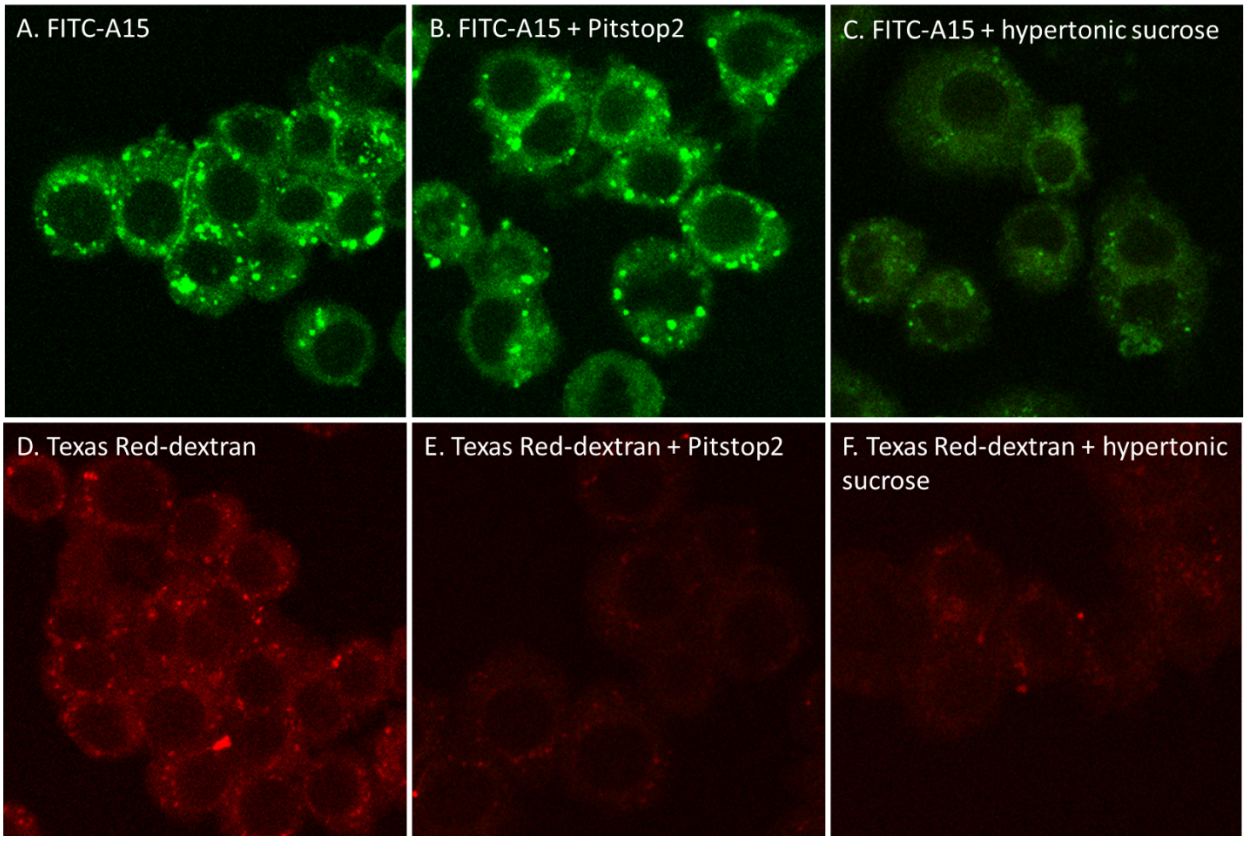

Figure 3.9. FITC-Alk staining following inhibition of clathrin-independent or clathrin-dependent endocytic pathways. RAW 264.7 cells were stained with FITC-Alk (A) or Texas Red-dextran (D) for 15 mins. Clathrin-independent and -dependent endocytosis was inhibited by pretreating cells with Pitstop 2 for 15 mins and staining with FITC-Alk (B) or Texas Red-dextran (E) for 15 mins. Clathrin-dependent endocytosis was inhibited by pretreating cells with 450mM hypertonic sucrose for 15 mins and staining with FITC-Alk (C) or Texas Red-dextran (F).

3.9 Changes in FITC-Alk staining upon cytochalasin D (CytD) treatment.

Endosome formation and trafficking is highly dependent on the cellular microfilament network (Anitei & Hoflack, 2011). We hypothesized therefore that accumulation of the FITC-Alk would be dependent on functioning microfilaments. To address this hypothesis, we utilized cytochalasin D (CytD), which disrupts microfilament networks by inhibiting the polymerization

of actin filaments (Stevenson & Begg, 1994). Cells were treated with 2 μM CytD for 1hr before staining with 50 μM FITC-Alk and 1μg/mL rhodamide-phallodin, a fluorescently labelled marker for f-actin. Cells treated with CytD displayed changes in microfilament architecture, as well as gross cell morphology, most likely as a result of loss of anchor filaments (**Figure 3.10 D**). While these cells did display some staining with the FITC-Alk, the bright cytoplasmic puncta were mostly absent indicating a dependence of these structures on functioning microfilaments (**Figure 3.10 E-F**). Instead FITC-Alk staining colocalized with large aggregates of f-actin found in the perinuclear region (**Figure 3.10 E-F**). These aggregates represent formation of microfilament bundles, comprised of mostly f-actin, that occur due to a CytD-induced contractile event (Schliwa, 1982). Interestingly, the small, pinpoints of FITC-Alk were unaffected by CytD treatment (**Figure 3.10 E-F**).

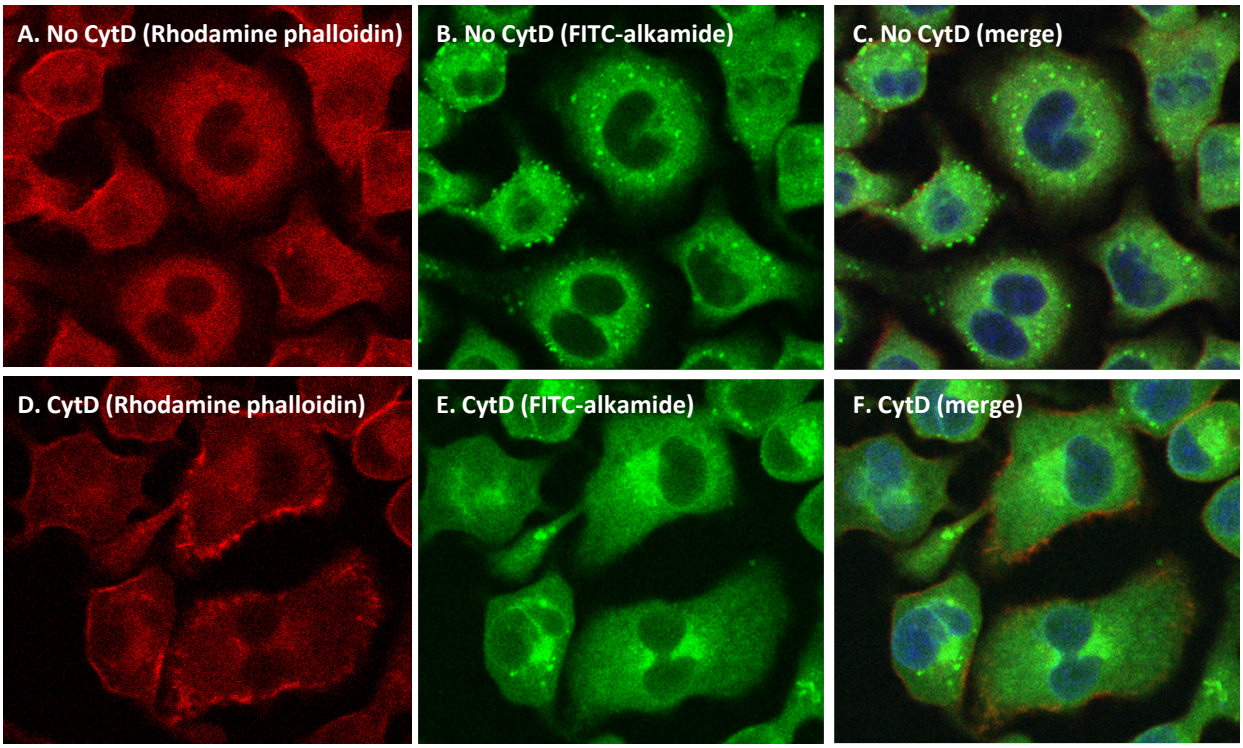

Figure 3.10. FITC-Alk staining in CytD treated cells. RAW 264.7 cells were either mock treated (A-C), or treated with 2 µM CytD for 1 hour before staining with 50 µM FITC-Alk for 15 min and fixed with 1 µg/mL rhodamine-phalloidin in 4% paraformaldehyde (D-F). DAPI was included in the mounting media to identify nuclei.

3.10 FITC-Alk staining compared to common endosomal pathway markers.

Several stages of maturation are recognized as endosomes move through the intracellular pathway. Therefore, antibodies to stage-specific markers were used to identify the endosome stage of FITC-Alk puncta. Included in these experiments were antibodies against early endosome markers caveolin-1, the clathrin heavy chain, and the early endosome antigen (EEA-1). We also examined the late-stage endosome marker Rab7 and the recycling endosome marker Rab-11. Unfortunately, as mentioned above, we were unable to perform double labeling experiments due to the detergent sensitivity of FITC-Alk staining and therefore we were limited to side-by-side

comparisons of staining patterns. Of these antibodies, only the antibody to the late-stage marker Rab7 produced a staining pattern similar to that of FITC-Alk, i.e., small, dispersed pinpoint staining together with large bright puncta, located in the perinuclear region with no specific orientation (**Figure 3.11 A vs. B**). In contrast, staining with antibodies against early endosome markers caveolin-1, clathrin heavy chanin, and EEA-1 produced staining patterns dissimilar to FITC-Alk (**Figure 3.11 A vs. C, D, and E**). Staining with an antibody to caveolin-1, an early endosomal marker and main structural component for caveolae in the plasma membrane (Okamoto 1998) resulted in 2-4 large bright aggregates per cell with smaller cytoplasmic puncta (**Figure 3.11 C**). Staining with an antibody to the clathrin heavy chain, which forms clathrin-coated vesicles arising from clathrin-coated pits (Rodriguez-Boulan et al 2005), resulted in puncta often on one side of the nucleus and also stained the cell periphery. (**Figure 3.11 D**) while the antibody to EEA-1 resulted in a staining pattern of numerous distinct small puncta dispersed throughout the cytoplasm (**Figure 3.11 E**). Finally, we evaluated the end-stages of the endosomal pathway using an antibody to Rab11, a marker for recycling endosomes. Rab11 produced a stain pattern that did not match FITC-Alk with very minimal staining throughout (**Figure 3.11 F**).

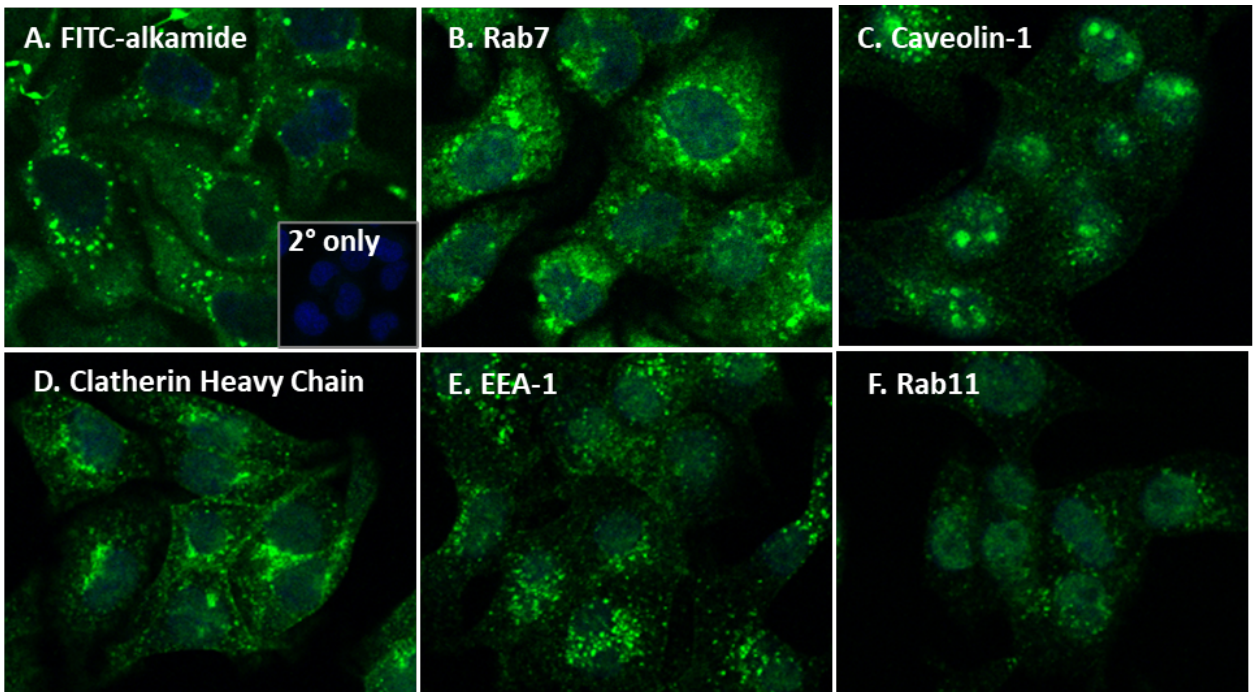

Figure 3.11. FITC-Alk staining compared with endosomal pathway markers. RAW 264.7 cells were stained with 50 μM FITC-Alk for 15 min and imaged as above (A). For immunofluorescence experiments, cells were fixed, permeabilized, and stained using antibodies against the indicated endosomal pathway markers. Cells were then stained with Alexa Fluor-488 labeled goat α-rabbit IgG secondary antibody and imaged using confocal microscopy (B-F). The inset in panel A shows staining with only secondary antibody and DAPI was added in the mounting media.

3.11 Alkamide structural requirements for uptake into cells

Finally, the effect of alkamide structure on uptake into cells was evaluated. Alkamide FITC-A-12 contains 12 carbons, similar to FITC-Alk, but does not have any double bonds in the fatty acid chain (**Figure 3.12 A & B**). FITC-A-8 and FITC-A-4 are shorter alkamides comparatively with eight and four carbons in the fatty acid chain, respectively, and no double bonds (**Figure 3.12 C & D**). Treating RAW 264.7 cells with the various alkamides resulted in

differences in measured fluorescence indicating differences in uptake efficacy, though all four fluorescently tagged alkamides were taken up by cells with significantly more fluorescence in all alkamide treatment groups compared to media alone. FITC-Alk and FITC-A-12 had a similar level of uptake with an average fluorescent unit (FU) of 302.93 and 311.40, respectively. FITC-A-8 displayed the highest levels of fluorescence with an average of 610.33 FU, which was significantly more than FITC-Alk, FITC-A-12, and FITC-A-4 ($p<0.0001$). FITC-A-4 treated cells had the lowest FU with an average of 181.20. These results indicate that double bonds are not required for uptake into cells as shown by the lack significant difference between FITC-Alk and FITC-A-12. In contrast, fatty acid chain length is important in mediating uptake of alkamides into cells. A fatty acid chain with 8 carbons was significantly better than both 12 and four carbons, with a four carbon chain being taken into cells with the lowest efficacy.

Figure 3.12. Alkamide structure influences cellular uptake. RAW 264.7 cells were treated with FITC-Alk (A) or 3 FITC-tagged analogs (B-D) for 15 minutes and fluorescence was measured via fluorimeter (E). Quantitative analysis showing differences in fluorescence units (FU) between treatments ± SEM (n=3) measured by one-way ANOVA with Tukey's posttest (E). ***significant difference between all treatments ($p<0.0006$), # significant difference between 1, 4, and 5 ($p<0.0026$), $ significant difference between 1, 3, and 5 ($p<0.0016$).

A.

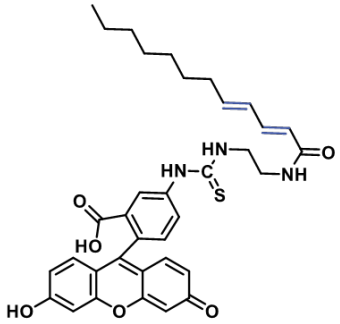

FITC-Alk

B.

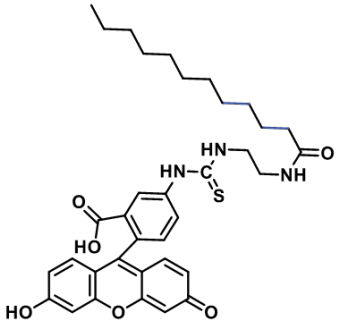

FITC-A-12

C.

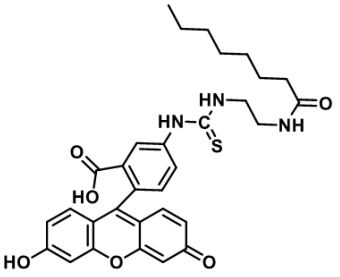

FITC-A-8

D.

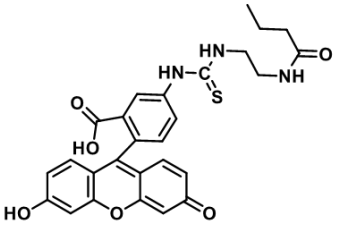

FITC-A-4

E.

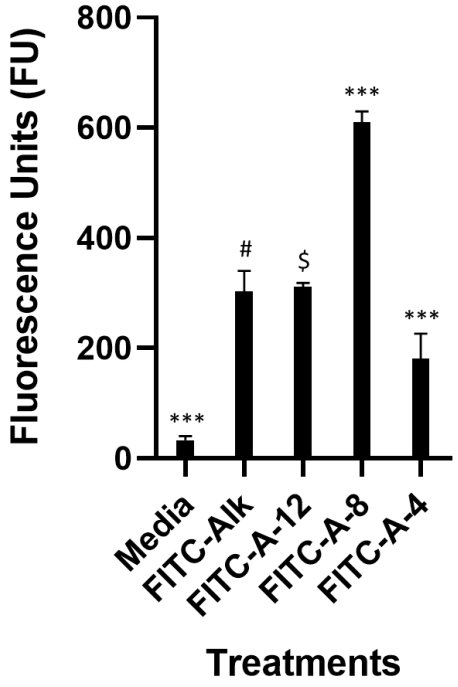

CHAPTER 4: DISCUSSION

In this study we evaluated the uptake of a fluorescently labeled alkamide by mammalian cells. Earlier studies from our lab indicated that the fatty acid, oxygen, and amide of this alkamide are essential for suppression of TNF-α production but that substitutions in the head group were tolerated while preserving activity (Moazami et al., 2015). Therefore, we replaced the head group on (2E,4E)-N-isobutyldodeca-2,4-dienamide with fluorescein isothiocyanate (FITC) to produce our fluorescent probe. The FITC-Alk molecule retained its ability to inhibit TNF-α production from LPS-stimulated RAW 264.7 cells, and therefore we moved forward with the FITC-Alk to study the intracellular transport of the alkamide. Our results showed that the FITC-Alk molecule was able to enter cells and entry was both time- and concentration-dependent. We observed FITC-Alk accumulation in the cytoplasm as both pinpoint foci and large puncta. This pattern was very similar in the three cell types tested, suggesting an uptake mechanism that is not tissue specific, and in this report, we focused on the identification of the large puncta. We also noted that the staining by FITC-Alk was detergent sensitive, even after fixation, limiting our use of antibodies in double labeling experiments.

Early on we examined a variety of cellular organelles including endoplasmic reticulum, Golgi apparatus, and mitochondria, and none of these produced a pattern of staining like the FITC-Alk pattern. Several lines of evidence lead us to conclude that the large puncta formed after FITC-Alk treatment represent endosomal vesicles. First, we found colocalization with fluorescently labeled dextran, a well-established marker for endosomal vesicles. We also found that high concentrations of dextran could compete with FITC-Alk and prevent formation of the large puncta. Fluorescent dextran has been shown to enter the endocytic pathway through non-specific micropinocytosis and receptor-mediated endocytosis (Z. Liu & Roche, 2015; Sallusto, Cella,

Danieli, & Lanzavecchia, 1995) and therefore both mechanisms may be responsible for FITC-Alk uptake. Then we sought to identify the mechanism for uptake of the alkamide by using inhibitors of various endocytic pathways, although their exact mechanisms of action are not fully understood. We found that inhibition of clathrin-mediated endocytosis with hypertonic sucrose blocked puncta formation as well as decreased overall staining intensity. Additionally, we found that puncta formation was dependent on an intact microfilament network, in accord with the established role for actin filaments in endosomal trafficking (Schliwa, 1982; Stevenson & Begg, 1994). Using 3D depth coding made from 3D reconstructions from Z-stacks, we found that the puncta were dispersed throughout the cells, without any orientation or polarization, also a characteristic of endosomes (Mellman, 1996). The nature of the small pinpoint staining following FITC-Alk treatment remains unclear. It is possible these small foci represent a different stage of endosome, or alternatively a different cellular organelle. It is also possible that the small foci arise from FITC-Alk escaping from endosomes and forming vesicles in the cytoplasm (Henry, El-Sayed, Pirie, Hoffman, & Stayton, 2006). Interestingly, formation of the small foci was resistant to treatment with CytD, indicating that their formation is independent of microfilament function.

Studies of the endosomal pathway have recognized several stages of endosome formation and maturation. Initially, regions of cell membrane are endocytosed in a microfilament-dependent manner to form early endosomes via clathrin-dependent or caveolin-dependent mechanisms (Elkin, Lakoduk, & Schmid, 2016; Lim & Gleeson, 2011). Early endosomes are characterized and identified by the protein EEA-1 which interacts with phosphatidylinositol 3-kinases and aids in endosome trafficking (Mills, Jones, & Clague, 1998; Patki et al., 1997). In this study, the pattern of staining with antibody markers for clathrin coated pits, caveolae, and early endosomes was not similar to the staining noted with FITC-Alk indicating that the large puncta are probably not early

endosomes. In the endosomal pathway, early endosomes move via microfilament transport, either through the recycling pathway or mature to late endosomes, which are ultimately degraded (Elkin et al., 2016; Huotari & Helenius, 2011). This process is regulated in part by Rab GTPases, which can be used as markers for the latter stages of the endosomal pathway (Rink, Ghigo, Kalaidzidis, & Zerial, 2005). Late endosomes are characterized by the expression of Rab7, which functions in endosome maturation and cargo sorting, while recycling endosomes express Rab11 (Girard et al., 2014; Huotari & Helenius, 2011; Takahashi et al., 2012). Rab7 has also been shown to play a role in endosome-lysosome transport (Wang, Ming, Xiaochun, & Hong, 2011). Our experiments with an antibody that recognizes the late endosomal protein Rab7 suggest that the large puncta formed following FITC-Alk treatment represent late endosomal vesicles. This conclusion is also supported by the perinuclear location of the puncta which is consistent with the intracellular position of late-stage endosomes (Neefjes, Jongsma, & Berlin, 2017). Most late-stage endosomes are trafficked to the perinuclear region of the cell where they fuse with lysosomes to generate endolysosomes and the contents undergo degradation (Huotari & Helenius, 2011). The FITC-Alk molecule seemed to accumulate in late endosomes with brightness increasing steadily over at least a 4 h period. It is possible therefore that the FITC-Alk could be blocking fusion of the late endosome with the lysosome and therefore accumulating in late endosomes. Alternatively, the uptake of the FITC-Alk could be resistant to degradation by RAW 264.7 cells or could exceed the degradative abilities of the cell and lead to accumulation in the late endosome. Degradation of alkamides has been shown to occur by liver microsomes (Nadja B. Cech et al., 2006), and RAW 264.7 cell may lack sufficient oxidative capacity to efficiently process the alkamide.

Endosomes serve multiple functions for the cell. They allow cells to internalize important molecules from the extracellular environment, facilitate recycling and degradation of

macromolecules, and participate in adhesion by regulating the transport of adhesion molecules to and from the cell surface (de Madrid, Greenberg, & Hatini, 2015; Scott, Vacca, & Gruenberg, 2014). Many pathogens have taken advantage of this vital cellular process to gain entry into the cell such as SARS-CoV, influenza virus, *Chlamydia* sp., *Shigella* sp., *Salmonella* sp., adeno-associated virus, and human papillomavirus (Allgood & Neunuebel, 2018; Matlin, Reggio, Helenius, & Simons, 1981; Popa-Wagner et al., 2012; Spoden et al., 2008). Recent studies have also shown that endosomes have important functions in cellular signaling pathways, such as the signal endosomes of neurons that carry cargo along microtubules, and in T cells where endosomes have been shown to carry key T cell secondary messengers (Benzing, Rossy, & Gaus, 2013; Schmieg, Menendez, Schiavo, & Terenzio, 2014). Additionally, TLR3 and TLR7 which recognize viral RNA in endosomes, signal from endosomes, as does TLR9 which recognizes CpG-rich DNA found in bacteria and viruses (Hipp et al., 2015; Matsumoto, Funami, Tatematsu, Azuma, & Seya, 2014; Petes, Odoardi, & Gee, 2017).

The accumulation of the FITC-Alk in endosomes raises the possibility that in addition to effects on cell surface receptors, alkamide activities may arise from their uptake into endosomes. Inhibition of the endosomal protein endothelin-converting enzyme-1 has been linked to pain inhibition, and therefore it is possible that the analgesic activity of alkamides may in part stem from endosomal signaling (Murphy, Padilla, Hasdemir, Cottrell, & Bunnett, 2009). Inhibition of clathrin-dependent and -independent endocytosis led us to conclude that the alkamide is mostly entering through clathrin-dependent endocytosis as cells treated with hypertonic sucrose had a decreased staining intensity as well as fewer bight puncta. Hypertonic sucrose traps the clathrin in microcages thereby inhibiting clathrin function (Dutta & Donaldson, 2012). Hypertonic sucrose exerts a relatively non-specific inhibitory effect, blocking receptor-mediated endocytosis, as well

as “non-coated” cell membrane invaginations, clathrin-coated pits, and interferes with fluid phase macropinocytosis (Carpentier et al., 1989). These findings allow us to conclude that clathrin is involved in the endocytosis of alkamides, but it does not allow us to elucidate the exact type of clathrin-dependent endocytosis taking place. Further, while staining intensity was reduced with hypertonic sucrose pretreatment, it was not completely abolished, perhaps indicating a second mechanism of entry, or alternatively, the inhibitory effect of sucrose was not complete. Other types of small molecules, such as low molecular weight dextran, are taken into cells through multiple mechanisms such as both macropinocytosis and micropinocytosis (L. Li et al., 2015). Therefore, it is possible that alkamides could be entering through multiple mechanisms, which could also explain the small pinpoint staining in the cytoplasm. In the future it will be important to resolve the pathways of alkamide entry into cells since they could be linked to intracellular activity.

The differences in cellular uptake based on structure could also explain the differences seen in biological activities of alkamides. In our experiments with alkamides using RAW 264.7 macrophages, we found that the number and placement of double bonds did not affect the activity A15 (Moazami et al., 2015). In contrast, the length of the fatty acid chain did impact activity with these cells, with fatty acid chains less than 12 carbons eliminating anti-inflammatory activity (Moazami et al., 2015). On the other hand, our experiments with mast cells revealed a bell-shaped activity curve with 8 carbons as most effective with lower levels of activity seen with both longer and shorter fatty acid chains (Collette 2017). It is possible therefore, that the effects we have noted with macrophages do occur at the cell surface but those effects noted with mast cells occur intracellularly where differential uptake directly affects cellular activity. Future experiments will be performed with mast cells to confirm that hypothesis.

Discovering that alkamides readily enter cells by endocytosis raises the possibility that they could be linked to other pharmacologically active compounds to enhance uptake into intracellular endosomal compartments. For example, large molecules designed to target the BCL-2 pathway often fail to exert effects due to their inability to cross the cell membrane and enter cells (Verdine & Walensky, 2007) and it has been proposed that "undruggable" targets may be reached if a drug is able to enter the endocytic pathway and escape before degradation (Pei & Buyanova, 2019). Similarly, the efficacy of drugs to treat Alzheimer's disease, certain cancers, and lysosomal storage diseases, could be improved if they were directed to the endolysosomal compartment (Bareford & Swaan, 2007). Linking the alkamide to larger molecules raises the possibility of delivering drugs to the endosomal compartment and potentially unlocking previously unreachable drug targets.

In summary, in this report we have shown that a fluorescent alkamide analog readily enters cells and likely accumulates in late endosomal vesicles, a novel finding in alkamide research. In addition to alkamide degradation, this intracellular location might be important for alkamide signaling. There are structure:function relationships for alkamide endocytosis with fatty acid chain length playing a vital role. The endosome localizing capability of this alkamide could also be used to transport therapeutic compounds into the endosomal pathway.

REFERENCES

Abdubakiev, S., Li, H., Lu, X., Li, J., & Aisa, H. A. (2020). N-Alkylamides from Piper longum L. and their stimulative effects on the melanin content and tyrosinase activity in B16 melanoma cells. *Natural product research, 34*(17), 2510-2513. doi:10.1080/14786419.2018.1539982

Albin, K. C., & Simons, C. T. (2010). Psychophysical evaluation of a sanshool derivative (alkylamide) and the elucidation of mechanisms subserving tingle. *PLoS One, 5*(3), e9520-e9520. doi:10.1371/journal.pone.0009520

Allgood, S. C., & Neunuebel, M. R. (2018). The recycling endosome and bacterial pathogens. *Cellular microbiology, 20*(7), e12857-n/a. doi:10.1111/cmi.12857

Anitei, M., & Hoflack, B. (2011). Bridging membrane and cytoskeleton dynamics in the secretory and endocytic pathways. *Nature cell biology, 14*(1), 11-19. doi:10.1038/ncb2409

Arango Duque, G., & Descoteaux, A. (2014). Macrophage Cytokines: Involvement in Immunity and Infectious Diseases. *Frontiers in immunology, 5*, 491-491. doi:10.3389/fimmu.2014.00491

Barbosa, A. F., Pereira, C. D. S. S., Mendes, M. F., De Carvalho Junior, R. N., De Carvalho, M. G., Maia, J. G. S., & Sabaa-Srur, A. U. O. (2017). Spilanthol Content in the Extract Obtained by Supercritical CO2at Different Storage Times of Acmella Oleracea L. *Journal of Food Process Engineering, 40*(3), e12441. doi:10.1111/jfpe.12441

Bareford, L., & Swaan, P. (2007). Endocytic mechanisms for targeted drug delivery. *Advanced drug delivery reviews, 59*(8), 748-758. doi:10.1016/j.addr.2007.06.008

Bautista, D. M., Sigal, Y. M., Milstein, A. D., Garrison, J. L., Zorn, J. A., Tsuruda, P. R., . . . Julius, D. (2008). Pungent agents from Szechuan peppers excite sensory neurons by inhibiting two-pore potassium channels. *Nature Neuroscience, 11*(7), 772-779. doi:http://dx.doi.org/10.1038/nn.2143

Benzing, C., Rossy, J., & Gaus, K. (2013). Do signalling endosomes play a role in T cell activation? *The FEBS journal, 280*(21), 5164-5176. doi:10.1111/febs.12427

Boonen, J., Bronselaer, A., Nielandt, J., Veryser, L., De Tré, G., & De Spiegeleer, B. (2012). Alkamid database: Chemistry, occurrence and functionality of plant N-alkylamides. *J Ethnopharmacol, 142*(3), 563-590. doi:10.1016/j.jep.2012.05.038

Bryant, B. P., & Mezine, I. (1999). Alkylamides that produce tingling paresthesia activate tactile and thermal trigeminal neurons. *Brain research, 842*(2), 452-460. doi:10.1016/S0006-8993(99)01878-8

Carpentier, J.-L., Sawano, F., Geiger, D., Gorden, P., Perrelet, A., & Orci, L. (1989). Potassium depletion and hypertonic medium reduce ?non-coated? and clathrin-coated pit formation, as well as endocytosis through these two gates. *Journal of cellular physiology, 138*(3), 519-526. doi:10.1002/jcp.1041380311

Cech, N. B., Kandhi, V., Davis, J. M., Hamilton, A., Eads, D., & Laster, S. M. (2010). Echinacea and its alkylamides: effects on the influenza A-induced secretion of cytokines, chemokines, and PGE_2 from RAW 264.7 macrophage-like cells. *Int Immunopharmacol, 10*(10), 1268-1278. doi:10.1016/j.intimp.2010.07.009

Cech, N. B., Tutor, K., Doty, B. A., Spelman, K., Sasagawa, M., Raner, G. M., & Wenner, C. A. (2006). Liver enzyme-mediated oxidation of Echinacea purpurea alkylamides: production of novel metabolites and changes in immunomodulatory activity. *Planta medica, 72*(15), 1372-1377. Retrieved from http://ncsu.summon.serialssolutions.com/2.0.0/link/0/eLvHCXMwpV1La9tAEF7apodc-nAeTZu0c_LJqqXVa91LSYNNCznk4EBuZrU7Cya25KC0VP0L_dOdWUnYBEIOvQg dtLAwo9GH9nsIEcvPYfBgJhiT6YlySV5QAxmDYWYjE0mdWRtZ4wXfO_922thTlsZ 05e6npB_dtjL813ycKU6JiMKvm7uAU6T4tLWL1Hgu9thojil--c32VCGZdJKUWAbMqHscVfqvy-y1uO034kklHGWwy64fe0dDb2PRuzf-x6bfiFcdCIXztmveimdYDsTLbxUBxWYghletnXUzgvlWnVWPYAhXW6Pr5kD8vWR SB2D5p1lj4DUohF-h-r1sg5qgcjBlrqY2qGFDJWUKPOjVbUN9uLRYf4FN6zjbPV1Wv3AFa7yn1mRxdA26tN CKk2tYlrBkOUu1pjUrTw8A1mVw_MWhuJ5N5xffgy7cITAx4YLAhZEyec5-fiZVhAMxKaLcESCxaLSx7GvnZKp0qLRReZFNJKZapoXVKsTcyCPxoqxKfCcgTbMi zqzStDbRsqAb51wiDVqdoItOxKe-Fgt6efhERJdY_awXfTVOxHFb_cWm9fhYsMtQEib5-yfXfhD7sgszCqNTsedobOAZbY6a5KPvP7pOf8z-AbgX9Ow

Chen, L., Long, C., Nguyen, J., Kumar, D., & Lee, J. (2018). Discovering alkylamide derivatives of bexarotene as new therapeutic agents against triple-negative breast cancer. *Bioorg Med Chem Lett, 28*(3), 420-424. doi:10.1016/j.bmcl.2017.12.033

Cieśla, Ł., & Moaddel, R. (2016). Comparison of analytical techniques for the identification of bioactive compounds from natural products. *Natural product reports, 33*(10), 1131-1145. doi:10.1039/c6np00016a

Clifford, L. J., Nair, M. G., Rana, J., & Dewitt, D. L. (2002). Bioactivity of alkamides isolated from Echinacea purpurea (L.) Moench. *Phytomedicine (Stuttgart), 9*(3), 249-253. doi:10.1078/0944-7113-00105

Cline, T. D., Beck, D., & Bianchini, E. (2017). Influenza virus replication in macrophages: balancing protection and pathogenesis. *Journal of general virology, 98*(10), 2401-2412. doi:10.1099/jgv.0.000922

Dallazen, J. L., Maria-Ferreira, D., da Luz, B. B., Nascimento, A. M., Cipriani, T. R., de Souza, L. M., . . . de Paula Werner, M. F. (2020). Pharmacological potential of alkylamides from

Acmella oleracea flowers and synthetic isobutylalkyl amide to treat inflammatory pain. *Inflammopharmacology, 28*(1), 175-186. doi:10.1007/s10787-019-00601-9

Dallazen, J. L., Maria-Ferreira, D., da Luz, B. B., Nascimento, A. M., Cipriani, T. R., de Souza, L. M., . . . de Paula Werner, M. F. (2018). Distinct mechanisms underlying local antinociceptive and pronociceptive effects of natural alkylamides from Acmella oleracea compared to synthetic isobutylalkyl amide. *Fitoterapia, 131*, 225-235. doi:10.1016/j.fitote.2018.11.001

de Madrid, B. H., Greenberg, L., & Hatini, V. (2015). RhoGAP68F controls transport of adhesion proteins in Rab4 endosomes to modulate epithelial morphogenesis of Drosophila leg discs. *Developmental biology, 399*(2), 283-295. doi:10.1016/j.ydbio.2015.01.004

de Souza, G. C., Viana, M. D., Goés, L. D. M., Sanchez-Ortiz, B. L., Silva, G. A. d., Pinheiro, W. B. d. S., . . . Carvalho, J. C. T. (2019). Reproductive toxicity of the hydroethanolic extract of the flowers of Acmella oleracea and spilanthol in zebrafish: In vivo and in silico evaluation. *Human & experimental toxicology, 39*(2), 127-146. doi:10.1177/0960327119878257

Dubey, S., Maity, S., Singh, M., Saraf, S. A., & Saha, S. (2013). Phytochemistry, Pharmacology and Toxicology of Spilanthes acmella: A Review. *Advances in pharmacological sciences, 2013*, 423750-423750. doi:10.1155/2013/423750

Dubin, A. E., & Patapoutian, A. (2010). Nociceptors: the sensors of the pain pathway. *The Journal of clinical investigation, 120*(11), 3760-3772. doi:10.1172/jci42843

Dutta, D., & Donaldson, J. G. (2012). Search for inhibitors of endocytosis: Intended specificity and unintended consequences. *Cellular logistics, 2*(4), 203-208. doi:10.4161/cl.23967

Ee, G. C. L., Lim, C. M., Rahmani, M., Shaari, K., & Bong, C. F. J. (2010). Pellitorine, a Potential Anti-Cancer Lead Compound against HL60 and MCT-7 Cell Lines and Microbial Transformation of Piperine from Piper Nigrum. *Molecules (Basel, Switzerland), 15*(4), 2398-2404. doi:10.3390/molecules15042398

Elkin, S. R., Lakoduk, A. M., & Schmid, S. L. (2016). Endocytic pathways and endosomal trafficking: a primer. *Wiener medizinische Wochenschrift, 166*(7-8), 196-204. doi:10.1007/s10354-016-0432-7

Elufioye, T. O., Habtemariam, S. and Adejare, A. . (2020). Chemistry and Pharmacology of Alkylamides from Natural Origin. *Revista brasileira de farmacognosia*, 1-19. doi:10.1007/s43450-020-00095-5

Fan Yang Jie, Z. (2017). Understand spiciness： mechanism of TRPV1 channel activation by capsaicin. *Protein & cell, 8*(3), 169-177. doi:10.1007/s13238-016-0353-7

Faulk, D. M., & Badylak, S. F. (2014). Chapter 8 - Natural Biomaterials for Regenerative Medicine Applications. In (pp. 101-112): Elsevier Inc.

Gerhold, K. A., & Bautista, D. M. (2010). Tingling Alkylamides from Echinacea Activate Somatosensory Neurons. *Biophysical journal, 98*(3), 496. doi:10.1016/j.bpj.2009.12.2701

Gertsch, J. (2008). Immunomodulatory lipids in plants: plant fatty acid amides and the human endocannabinoid system. *Planta medica, 74*(6), 638-650. doi:10.1055/s-2008-1034302

Gertsch, J., Schoop, R., Kuenzle, U., & Suter, A. (2004). Echinacea alkylamides modulate TNF-α gene expression via cannabinoid receptor CB2 and multiple signal transduction pathways. *FEBS letters, 577*(3), 563-569. doi:10.1016/j.febslet.2004.10.064

Ghassempour, A., Noruzi, M., Zandehzaban, M., Talebpour, Z., Yari Khosroshahi, A., Najafi, N. M., . . . Aboul-Enein, H. Y. (2007). Purification of Paclitaxel Isolated from Taxus baccata L. Cell Culture by Microwave-Assisted Extraction and Two-Dimensional Liquid Chromatography. *Journal of liquid chromatography & related technologies, 31*(3), 382-394. doi:10.1080/10826070701780672

Girard, E., Chmiest, D., Fournier, N., Johannes, L., Paul, J.-L., Vedie, B., & Lamaze, C. (2014). Rab7 Is Functionally Required for Selective Cargo Sorting at the Early Endosome. *Traffic (Copenhagen, Denmark), 15*(3), 309-326. doi:10.1111/tra.12143

Gulledge, T. V., Collette, N. M., Mackey, E., Johnstone, S. E., Moazami, Y., Todd, D. A., . . . Laster, S. M. (2018). Mast cell degranulation and calcium influx are inhibited by an Echinacea purpurea extract and the alkylamide dodeca-2E,4E-dienoic acid isobutylamide. *J Ethnopharmacol, 212*, 166-174. doi:10.1016/j.jep.2017.10.012

Gulledge, T. V., Collette, N. M., Mackey, E., Johnstone, S. E., Moazami, Y., Todd, D. A., . . . Laster, S. M. (2018). Mast cell degranulation and calcium influx are inhibited by an Echinacea purpurea extract and the alkylamide dodeca-2E,4E-dienoic acid isobutylamide. *Journal of ethnopharmacology, 212*, 166-174. doi:10.1016/j.jep.2017.10.012

Hajdu, Z., Nicolussi, S., Rau, M., Lorántfy, L. s., Forgo, P., Hohmann, J., . . . Gertsch, J. r. (2014). Identification of Endocannabinoid System-Modulating N-Alkylamides from Heliopsis helianthoides var. scabra and Lepidium meyenii. *Journal of natural products (Washington, D.C.), 77*(7), 1663-1669. doi:10.1021/np500292g

Harpalani, A. D., Snyder, S. W., Subramanyam, B., Egorin, M. J., & Callery, P. S. (1993). Alkylamides as inducers of human leukemia cell differentiation: a quantitative structure-activity relationship study using comparative molecular field analysis. *Cancer research (Chicago, Ill.), 53*(4), 766-771. Retrieved from http://ncsu.summon.serialssolutions.com/2.0.0/link/0/eLvHCXMwnZ1NT9tAEIZXhEPFBZUWVCjQOfViOUr8tQsShygK6oG2EiQSN2vxjkVE4qB8HPg1_FVmvxw3CNH2YkWWsrL3WY3H63feYSyO2p1wIyZ0OT2JROdMpFiklOIqVaCgh7uxO-cl39jb8U0739O0_x9nOkekdd3sP7CuB6UT9JuI05GY0_GvqPcmD0_EeKxwoTvI0I0RurmRa9hufBNcPeB0LAO9Y1-3R1mOa5GH1HWWlSk906Ii6y-7mmOoKyBMo4m5189pnZexpw1Wvna3dhKf-ra7gdHIBdKZnzST4b5ecfPA-Q3dmw_KVhliItdk0vb7FMrV6emPwaEtzKxDrQjTxPblaeM6uvLE-kf68Gu9gt0ySxqxlGdZ47HMbaeWPx2zf_3OL0dXV_lwcDv8ru9wqsbF8gKrcHTTYi2KX3r_pn-

9Fv04Uau_uDfeKzKXXww_sl33YgA9y3SPbWH1iX346aQPn9lzAy3IBXi0MCvBoAW
PFjRa2EB7DhKaYOE1WGiCBQMWDFhogIUaLBiw4MHus9HlYNj_EbruGmGXkr4kj
KIyQ8klClGmZVJgJ42UoOy0E0dFTHllJKSIjB1_yhHpVaGQiiuVyiwT0RnGB2y7mlX
4hUGsu5p1C0p972ggSaNkpZJp0S0p3UyS-
JB987OcU_TSsyArnK0WOadgoL0YDtmBnfz80Zqs5MI4AWZH7_71K9tZr79jtk2zhyd
0aRQtTlmL34pTswReABpbeLs

Henry, S. M., El-Sayed, M. E. H., Pirie, C. M., Hoffman, A. S., & Stayton, P. S. (2006). pH-Responsive Poly(styrene-alt-maleic anhydride) Alkylamide Copolymers for Intracellular Drug Delivery. *Biomacromolecules, 7*(8), 2407-2414. doi:10.1021/bm060143z

Heuser, J. E., & Anderson, R. G. (1989). Hypertonic media inhibit receptor-mediated endocytosis by blocking clathrin-coated pit formation. *The Journal of cell biology, 108*(2), 389-400. doi:10.1083/jcb.108.2.389

Hipp, M. M., Shepherd, D., Booth, S., Waithe, D., Reis e Sousa, C., & Cerundolo, V. (2015). The Processed Amino-Terminal Fragment of Human TLR7 Acts as a Chaperone To Direct Human TLR7 into Endosomes. *The Journal of immunology (1950), 194*(11), 5417-5425. doi:10.4049/jimmunol.1402703

Hobro, A. J., & Smith, N. I. (2017). An evaluation of fixation methods: Spatial and compositional cellular changes observed by Raman imaging. *Vibrational spectroscopy, 91*, 31-45. doi:10.1016/j.vibspec.2016.10.012

Huang, W.-C., Huang, C.-H., Hu, S., Peng, H.-L., & Wu, S.-J. (2019). Topical Spilanthol Inhibits MAPK Signaling and Ameliorates Allergic Inflammation in DNCB-Induced Atopic Dermatitis in Mice. *International journal of molecular sciences, 20*(10), 2490. doi:10.3390/ijms20102490

Huotari, J., & Helenius, A. (2011). Endosome maturation. *The EMBO journal, 30*(17), 3481-3500. doi:10.1038/emboj.2011.286

Ji, H. F., Li, X. J., & Zhang, H. Y. (2009). Natural products and drug discovery. Can thousands of years of ancient medical knowledge lead us to new and powerful drug combinations in the fight against cancer and dementia? *EMBO Rep, 10*(3), 194-200. doi:10.1038/embor.2009.12

Kindscher, K. (2016). The Uses of Echinacea angustifolia and Other Echinacea Species by Native Americans. In (pp. 9-20). Cham: Springer International Publishing.

Krystel-Whittemore, M., Dileepan, K. N., & Wood, J. G. (2016). Mast Cell: A Multi-Functional Master Cell. *Frontiers in immunology, 6*, 620-620. doi:10.3389/fimmu.2015.00620

Kumar, B. V., Connors, T. J., & Farber, D. L. (2018). Human T Cell Development, Localization, and Function throughout Life. *Immunity (Cambridge, Mass.), 48*(2), 202-213. doi:10.1016/j.immuni.2018.01.007

Kumar, S., Kamboj, J., Suman, & Sharma, S. (2011). Overview for various aspects of the health benefits of Piper longum linn. fruit. *Journal of acupuncture and meridian studies U6 - ctx_ver=Z39.88-2004&ctx_enc=info%3Aofi%2Fenc%3AUTF-8&rfr_id=info%3Asid%2Fsummon.serialssolutions.com&rft_val_fmt=info%3Aofi%2Ffmt%3Akev%3Amtx%3Ajournal&rft.genre=article&rft.atitle=Overview+for+various+aspects+of+the+health+benefits+of+Piper+longum+linn.+fruit&rft.jtitle=Journal+of+acupuncture+and+meridian+studies&rft.date=2011-06-01&rft.eissn=2093-8152&rft.volume=4&rft.issue=2&rft.spage=134&rft.epage=140&rft_id=info:doi/10.1016%2FS2005-2901%2811%2960020-4&rft.externalDBID=NO_FULL_TEXT&paramdict=en-US U7 - Journal Article, 4*(2), 134-140. doi:10.1016/S2005-2901(11)60020-4

Lavin, Y., Mortha, A., Rahman, A., & Merad, M. (2015). Regulation of macrophage development and function in peripheral tissues. *Nature reviews. Immunology, 15*(12), 731-744. doi:10.1038/nri3920

Leporatti, M. L., & Ghedira, K. (2009). Comparative analysis of medicinal plants used in traditional medicine in Italy and Tunisia. *Journal of ethnobiology and ethnomedicine, 5*(1), 8-31. doi:10.1186/1746-4269-5-31

Ley, J. P., Krammer, G., Looft, J., Reinders, G., & Bertram, H.-J. (2006). Structure-activity relationships of trigeminal effects for artificial and naturally occurring alkamides related to spilanthol. In (Vol. 43, pp. 21-24).

Li, L., Wan, T., Wan, M., Liu, B., Cheng, R., & Zhang, R. (2015). The effect of the size of fluorescent dextran on its endocytic pathway. *Cell biology international, 39*(5), 531-539. doi:10.1002/cbin.10424

Li, Y., Fang, F., Wei, J., Wu, X., Cui, R., Li, G., . . . Tan, D. (2019). Humic Acid Fertilizer Improved Soil Properties and Soil Microbial Diversity of Continuous Cropping Peanut: A Three-Year Experiment. *Scientific reports, 9*(1), 12014-12019. doi:10.1038/s41598-019-48620-4

Lim, J. P., & Gleeson, P. A. (2011). Macropinocytosis: an endocytic pathway for internalising large gulps. *Immunology and cell biology, 89*(8), 836-843. doi:10.1038/icb.2011.20

Liu, Y., Yadev, V. R., Aggarwal, B. B., & Nair, M. G. (2010). Inhibitory Effects of Black Pepper (Piper Nigrum) Extracts and Compounds on Human Tumor Cell Proliferation, Cyclooxygenase Enzymes, Lipid Peroxidation and Nuclear Transcription Factor-kappa-B. *Natural product communications, 5*(8), 1934578X1000500. doi:10.1177/1934578x1000500822

Liu, Z., & Roche, P. A. (2015). Macropinocytosis in phagocytes: regulation of MHC class-II-restricted antigen presentation in dendritic cells. *Frontiers in physiology, 6*, 1-1. doi:10.3389/fphys.2015.00001

Matlin, K. S., Reggio, H., Helenius, A., & Simons, K. (1981). Infectious Entry Pathway of Influenza Virus in a Canine Kidney Cell Line. *The Journal of cell biology, 91*(3), 601-613. doi:10.1083/jcb.91.3.601

Matsumoto, M., Funami, K., Tatematsu, M., Azuma, M., & Seya, T. (2014). Assessment of the Toll-Like Receptor 3 Pathway in Endosomal Signaling. In (Vol. 535, pp. 149-165). United States: Elsevier Science & Technology.

Matthias, A., Blanchfield, J. T., Penman, K. G., Toth, I., Lang, C. S., Voss, J. J., & Lehmann, R. P. (2004). Permeability studies of alkylamides and caffeic acid conjugates from echinacea using a Caco-2 cell monolayer model. *Journal of clinical pharmacy and therapeutics, 29*(1), 7-13. doi:10.1046/j.1365-2710.2003.00530.x

Mazzari, S., Canella, R., Petrelli, L., Marcolongo, G., & Leon, A. (1996). N-(2-Hydroxyethyl)hexadecanamide is orally active in reducing edema formation and inflammatory hyperalgesia by down-modulating mast cell activation. *European journal of pharmacology, 300*(3), 227-236. doi:10.1016/0014-2999(96)00015-5

McDonnell, A. M., & Dang, C. H. (2013). Basic review of the cytochrome p450 system. *Journal of the advanced practitioner in oncology, 4*(4), 263-268. doi:10.6004/jadpro.2013.4.4.7

Mellman, I. (1996). ENDOCYTOSIS AND MOLECULAR SORTING. *Annual review of cell and developmental biology, 12*(1), 575-625. doi:10.1146/annurev.cellbio.12.1.575

Menozzi-Smarrito, C., Riera, C. E., Munari, C., Le Coutre, J., & Robert, F. (2009). Synthesis and Evaluation of New Alkylamides Derived from α-Hydroxysanshool, the Pungent Molecule in Szechuan Pepper. *Journal of agricultural and food chemistry, 57*(5), 1982-1989. doi:10.1021/jf803067r

Mills, I. G., Jones, A. T., & Clague, M. J. (1998). Involvement of the endosomal autoantigen EEA1 in homotypic fusion of early endosomes. *Current biology, 8*(15), 881-884. doi:10.1016/S0960-9822(07)00351-X

Miyakado, M., Nakayama, I., Yoshioka, H., & Nakatani, N. (1979). The Piperaceae Amides I: Structure of Pipercide, A New Insecticidal Amide from Piper nigrum L. *Agricultural and biological chemistry, 43*(7), 1609-1611. doi:10.1080/00021369.1979.10863675

Moazami, Y., Gulledge, T. V., Laster, S. M., & Pierce, J. G. (2015). Synthesis and biological evaluation of a series of fatty acid amides from Echinacea. *Bioorg Med Chem Lett, 25*(16), 3091-3094. doi:10.1016/j.bmcl.2015.06.024

Modarai, M., Gertsch, J., Suter, A., Heinrich, M., & Kortenkamp, A. (2007). Cytochrome P450 inhibitory action of Echinacea preparations differs widely and co-varies with alkylamide content. *Journal of pharmacy and pharmacology, 59*(4), 567-573. doi:10.1211/jpp.59.4.0012

Modarai, M., Silva, E., Suter, A., Heinrich, M., & Kortenkamp, A. (2010). Safety of Herbal Medicinal Products: Echinacea and Selected Alkylamides Do Not Induce CYP3A4

mRNA Expression. *Evidence-based complementary and alternative medicine, 2011*, 213021-213027. doi:10.1093/ecam/nep174

Molinatorres, J., Salgado-Garciglia, R., Ramirez-Chavez, E., & Del Rio, R. E. (1996). Purely olefinic alkamnides in Heliopsis longipes and Acmella (Spilanthes) oppositifolia. *Biochemical systematics and ecology, 24*(1), 43-47. doi:10.1016/0305-1978(95)00099-2

Morazzoni, P., Cristoni, A., Di Pierro, F., Avanzini, C., Ravarino, D., Stornello, S., . . . Musso, T. (2005). In vitro and in vivo immune stimulating effects of a new standardized Echinacea angustifolia root extract (Polinacea™). *Fitoterapia, 76*(5), 401-411. doi:10.1016/j.fitote.2005.02.001

Murphy, J. E., Padilla, B. E., Hasdemir, B., Cottrell, G. S., & Bunnett, N. W. (2009). Endosomes: A legitimate platform for the signaling train. *Proceedings of the National Academy of Sciences - PNAS, 106*(42), 17615-17622. doi:10.1073/pnas.0906541106

Neefjes, J., Jongsma, M. M. L., & Berlin, I. (2017). Stop or Go? Endosome Positioning in the Establishment of Compartment Architecture, Dynamics, and Function. *Trends in cell biology, 27*(8), 580-594. doi:10.1016/j.tcb.2017.03.002

O'Neill, J., Brock, C., Olesen, A. E., Andresen, T., Nilsson, M., & Dickenson, A. H. (2012). Unravelling the Mystery of Capsaicin: A Tool to Understand and Treat Pain. *Pharmacological Reviews, 64*(4), 939-971. doi:10.1124/pr.112.006163

Oláh, A., Szabó-Papp, J., Soeberdt, M., Knie, U., Dähnhardt-Pfeiffer, S., Abels, C., & Bíró, T. (2017). Echinacea purpurea -derived alkylamides exhibit potent anti-inflammatory effects and alleviate clinical symptoms of atopic eczema. *Journal of dermatological science, 88*(1), 67-77. doi:10.1016/j.jdermsci.2017.05.015

Pardridge, W. M. (2005). The blood-brain barrier: Bottleneck in brain drug development. *NeuroRx, 2*(1), 3-14. doi:10.1602/neurorx.2.1.3

Park, I.-K. (2012). Insecticidal activity of isobutylamides derived from Piper nigrum against adult of two mosquito species, Culex pipiens pallens and Aedes aegypti. *Natural product research U6 - ctx_ver=Z39.88-2004&ctx_enc=info%3Aofi%2Fenc%3AUTF-8&rfr_id=info%3Asid%2Fsummon.serialssolutions.com&rft_val_fmt=info%3Aofi%2Ffmt%3Akev%3Amtx%3Ajournal&rft.genre=article&rft.atitle=Insecticidal+activity+of+isobutylamides+derived+from+Piper+nigrum+against+adult+of+two+mosquito+species%2C+Culex+pipiens+pallens+and+Aedes+aegypti&rft.jtitle=Natural+product+research&rft.date=2012-01-01&rft.eissn=1478-6427&rft.volume=26&rft.issue=22&rft.spage=2129&rft.epage=2131&rft_id=info:doi/10.1080%2F14786419.2011.628178&rft.externalDBID=NO_FULL_TEXT&paramdict=en-US U7 - Journal Article, 26*(22), 2129-2131. doi:10.1080/14786419.2011.628178

Parsons, J. L., Cameron, S. I., Harris, C. S., & Smith, M. L. (2018). Echinacea biotechnology: advances, commercialization and future considerations. *Pharmaceutical Biology, 56*(1). Retrieved from

https://proxying.lib.ncsu.edu/index.php/login?url=https://www.proquest.com/docview/2351040668?accountid=12725

http://JS8LB8FT5Y.search.serialssolutions.com/directLink?&atitle=Echinacea+biotechnology%3A+advances%2C+commercialization+and+future+considerations&author=Parsons%2C+Jessica+L%3BCameron%2C+Stewart+I%3BHarris%2C+Cory+S%3BSmith%2C+Myron+L&issn=13880209&title=Pharmaceutical+Biology&volume=56&issue=1&date=2018-12-01&spage=&id=doi:&sid=ProQ_ss&genre=article

Patil, J. G., Ahire, M. L., Nitnaware, K. M., Panda, S., Bhatt, V. P., Kishor, P. B. K., & Nikam, T. D. (2012). In vitro propagation and production of cardiotonic glycosides in shoot cultures of Digitalis purpurea L. by elicitation and precursor feeding. *Applied microbiology and biotechnology, 97*(6), 2379-2393. doi:10.1007/s00253-012-4489-y

Patki, V., Virbasius, J., Lane, W. S., Toh, B.-H., Shpetner, H. S., & Corvera, S. (1997). Identification of an Early Endosomal Protein Regulated by Phosphatidylinositol 3-Kinase. *Proceedings of the National Academy of Sciences - PNAS, 94*(14), 7326-7330. doi:10.1073/pnas.94.14.7326

Paulraj, J., Govindarajan, R., & Palpu, P. (2013). The genus spilanthes ethnopharmacology, phytochemistry, and pharmacological properties: a review. *Adv Pharmacol Sci, 2013*, 510298. doi:10.1155/2013/510298

Pawlus, A. D., Freund, D. M., Gentile, C., Munter, D., Starr, E., Kegley, S., . . . Hegeman, A. D. (2014). *Chemical profiles of American prickly ash, botanical dietary supplements from the Zanthoxylum genera*.

Pei, D., & Buyanova, M. (2019). Overcoming Endosomal Entrapment in Drug Delivery. *Bioconjugate chemistry, 30*(2), 273-283. doi:10.1021/acs.bioconjchem.8b00778

Percival, S. S. (2000). Use of echinacea in medicine. *Biochemical pharmacology, 60*(2), 155-158. doi:10.1016/S0006-2952(99)00413-X

Petes, C., Odoardi, N., & Gee, K. (2017). The Toll for Trafficking: Toll-Like Receptor 7 Delivery to the Endosome. *Frontiers in immunology, 8*, 1075-1075. doi:10.3389/fimmu.2017.01075

Pilna, J., Vlkova, E., Krofta, K., Nesvadba, V., Rada, V., & Kokoska, L. (2015). In vitro growth-inhibitory effect of ethanol GRAS plant and supercritical CO2 hop extracts on planktonic cultures of oral pathogenic microorganisms. *Fitoterapia, 105*, 260-268. doi:10.1016/j.fitote.2015.07.016

Popa-Wagner, R., Porwal, M., Kann, M., Reuss, M., Weimer, M., Florin, L., & Kleinschmidt, J. A. (2012). Impact of VP1-Specific Protein Sequence Motifs on Adeno-Associated Virus Type 2 Intracellular Trafficking and Nuclear Entry. *Journal of virology, 86*(17), 9163-9174. doi:10.1128/jvi.00282-12

Prachayasittikul, V., Prachayasittikul, S., Ruchirawat, S., & Prachayasittikul, V. (2013). High therapeutic potential of Spilanthes acmella: A review. *EXCLI journal, 12*, 291-312. Retrieved from http://ncsu.summon.serialssolutions.com/2.0.0/link/0/eLvHCXMwnV1Li9swEBbdHEovy26f2W0X9RxcFPmpQA9h2dJCe2myJbcgyTIJSWyTxJT--52xZMcsSV8XYyQjC31oNDOamY8Qn39g3iOZEMCEkW01SwFlE8aKx0KpWGaR8tEV98i305Bv_imm_f9whjZAGvNm_wHrdlBogHdAHJ6AOTz_CnUM2xh0cqoGZbHHeCCrck7K5RpWcmF2A6k3GPdkE9O3hwuCxkk_u_36ZdD9JYrPrdQL-Uvu8FpjVdXO4x_mYNIf659UpVxXbTrQd-Re2cqfspb9k2Kzk6vfDg8fl4U7XZ1zwmaVOkkaDYce6BOuzvWRtkb88q78tNRdHaTKTQ0Vj5lAsvfDsdUGE7ZdWCx9ky71_qPJvfsJVjSAnsaDY0_nMGF19dd2KlgN2g1wwsgInLIxvSDnzkqgYwvwJXli8ufk6TcXB_GCjBBn2sGZtjjTIqMHnKnDeUTH1KL8ktx_upvefvYcC4YHqpgYemAQhyaKOUtVyrNU-ElkNJj1mmXM4PGABYe4NjqNmEDymERkCrRUFQZRZmB_vSK9vMjNG0L9EIxbpBjQoQp0yEWgWKKjII0Fk7EWffK-WYA5SBm8OpK5KardfAiKZOIHYJz2yWu7MvPSlkOZN8t3dbLnmjzjNYsIeq7ekt5-W5l3MCvY0DfkLJ4lNzVGD7s9TfQ

Qiang, Z., Hauck, C., Murphy, P., Qu, L., Widrlechner, M. P., Reddy, M. B., & Hendrich, S. (2011). Permeability of Echinacea alkylamides and ketones across Caco-2 cell monolayers. *The FASEB journal, 25*, 609.618-609.618. doi:10.1096/fasebj.25.1_supplement.609.18

Raduner, S., Majewska, A., Chen, J. Z., Xie, X. Q., Hamon, J., Faller, B., . . . Gertsch, J. (2006). Alkylamides from Echinacea are a new class of cannabinomimetics. Cannabinoid type 2 receptor-dependent and -independent immunomodulatory effects. *J Biol Chem, 281*(20), 14192-14206. doi:10.1074/jbc.M601074200

Reeke, J. G. N., Becker, J. W., Cunningham, B. A., Wang, J. L., Yahara, I., & Edelman, G. M. (1975). Structure and function of concanavalin A. *Advances in experimental medicine and biology, 55*, 13-33. Retrieved from http://ncsu.summon.serialssolutions.com/2.0.0/link/0/eLvHCXMwpV1LS8QwEB7UBfHie3F95uilbpvdJM1JFtlFD57cg7eSV0GEtrrs_3cmbUUF8eAll1IYZpLJN498AzDhN2nywyfkznvErla4NC-1slOPuMQFVRqtDVfhe26nHXtKT2M6c_deMrpuXzvKmo9zriWRudw2bwlNkaJqazdSYxMGRDRHLX7q-bOqIBSX7QQ96uwSOv8dVcbbZbEHr70gsamERhl87a4fR0bDSGPRszf-Q-h92O1AKJu1u-YANkJ1CNuPXZn9CK6fIqvs-j0wU3lGdx_Zj9Ulw_CZ-sRwf75UbHYMy8V8eXefdCMVkkYJmXguSonH1FnNnVcI3VKL-CegbjwGRqnNSo8mDYQLhQzc6RwtZFJrjfWIBPkQtqq6CifAzMRlKX7xQRkM8aRxHldEO3KSOUQ9I7jqFVDgjqUyhKlCvV4VvQpGMGxVXjQtsQZGI0LwqTz989cz2Mm0Em0q5BwGJR7VcIGyoWEuo81xnT8sPgCux7_7

Ren, T., Zhu, Y., & Kan, J. (2017). Zanthoxylum alkylamides activate phosphorylated AMPK and ameliorate glycolipid metabolism in the streptozotocin-induced diabetic rats. *Clinical and experimental hypertension (1993), 39*(4), 330-338. doi:10.1080/10641963.2016.1259332

Ren, T., Zhu, Y., Xia, X., Ding, Y., Guo, J., & Kan, J. (2017). Zanthoxylum alkylamides ameliorate protein metabolism disorder in STZ-induced diabetic rats. *Journal of molecular endocrinology, 58*(3), 113-125. doi:10.1530/JME-16-0218

Rink, J., Ghigo, E., Kalaidzidis, Y., & Zerial, M. (2005). Rab Conversion as a Mechanism of Progression from Early to Late Endosomes. *Cell (Cambridge), 122*(5), 735-749. doi:10.1016/j.cell.2005.06.043

Ross, S. H., & Cantrell, D. A. (2018). Signaling and Function of Interleukin-2 in T Lymphocytes. *Annual review of immunology, 36*(1), 411-433. doi:10.1146/annurev-immunol-042617-053352

Sailaja, R., & Setty, O. H. (2006). Protective effect of Phyllanthus fraternus against allyl alcohol-induced oxidative stress in liver mitochondria. *Journal of ethnopharmacology, 105*(1), 201-209. doi:10.1016/j.jep.2005.10.019

Sallusto, F., Cella, M., Danieli, C., & Lanzavecchia, A. (1995). Dendritic cells use macropinocytosis and the mannose receptor to concentrate macromolecules in the major histocompatibility complex class II compartment: downregulation by cytokines and bacterial products. *J Exp Med, 182*(2), 389-400. doi:10.1084/jem.182.2.389

Sasagawa, M., Cech, N. B., Gray, D. E., Elmer, G. W., & Wenner, C. A. (2006). Echinacea alkylamides inhibit interleukin-2 production by Jurkat T cells. *International immunopharmacology, 6*(7), 1214-1221. doi:10.1016/j.intimp.2006.02.003

Schliwa, M. (1982). Action of cytochalasin D on cytoskeletal networks. *The Journal of cell biology, 92*(1), 79-91. doi:10.1083/jcb.92.1.79

Schmieg, N., Menendez, G., Schiavo, G., & Terenzio, M. (2014). Signalling endosomes in axonal transport: Travel updates on the molecular highway. *Seminars in cell & developmental biology, 27*, 32-43. doi:10.1016/j.semcdb.2013.10.004

Schneider, E. M., & Sievers, A. (1981). Concanavalin A binds to the endoplasmic reticulum and the starch grain surface of root statocytes. *Planta, 152*(3), 177-180. doi:10.1007/BF00385141

Scott, C. C., Vacca, F., & Gruenberg, J. (2014). Endosome maturation, transport and functions. *Seminars in cell & developmental biology, 31*, 2-10. doi:10.1016/j.semcdb.2014.03.034

Shinde, S., Sebastian, J. K., Jain, J. R., Hanamanthagouda, M. S., & Murthy, H. N. (2016). Efficient in vitro propagation of Artemisia nilagirica var. nilagirica (Indian wormwood) and assessment of genetic fidelity of micropropagated plants. *Physiology and molecular biology of plants, 22*(4), 595-603. doi:10.1007/s12298-016-0379-6

Spelman, K., Depoix, D., McCray, M., Mouray, E., & Grellier, P. (2011). The traditional medicine Spilanthes acmella, and the alkylamides spilanthol and undeca-2E-ene-8,10-diynoic acid isobutylamide, demonstrate in vitro and in vivo anti-malarial activity. *Phytotherapy research, 25*(7), 1098-1101. doi:10.1002/ptr.3395

Spoden, G., Freitag, K., Husmann, M., Boller, K., Sapp, M., Lambert, C., & Florin, L. (2008). Clathrin- and Caveolin-Independent Entry of Human Papillomavirus Type 16—Involvement of Tetraspanin-Enriched Microdomains (TEMs). *PLoS One, 3*(10), e3313-e3313. doi:10.1371/journal.pone.0003313

Steinberg, K. M., Satyal, P., & Setzer, W. N. (2017). Bark Essential Oils of Zanthoxylum clava-herculis and Ptelea trifoliata: Enantiomeric Distribution of Monoterpenoids. *Natural product communications, 12*(6), 1934578. doi:10.1177/1934578X1701200632

Stevenson, B. R., & Begg, D. A. (1994). Concentration-dependent effects of cytochalasin D on tight junctions and actin filaments in MDCK epithelial cells. *Journal of cell science, 107 (Pt 3)*, 367-375. Retrieved from http://ncsu.summon.serialssolutions.com/2.0.0/link/0/eLvHCXMwnZ3PT9swFMetFWkSFwRs1QoDfNolypQ0cWwOO4y2CIluQ6KVeosc29FA4PAjHPjv956dph1SVeASJa4aufmkz8_Pft9HSNL_HoUvbILQBeqsi4gZ8OYiU0jWz5TWKpaaC1dOZTm2My_VuW5P-_s4QxuQxrzZN7BubwoNcA7E4QjM4fgq6gPMQrSNFG44r3BbL2_bUM91pf669EkbDN1iAU7Qg2sY4fy2OKffCucWVZukz4GDi1_DwXlg7jCJ4wbj7Bjzf1zh3OJnQTO6LgILXiF4vrOq3egf4-qutz_G28cUV3xjr9PSGtCIozscXNRBGx325jDxpTaakTXxNVL-F73-_Sc_nY7H-WQ0m3xDufNbfaXqH8aG08sO6YAJwhDM4KQdXuH9aerw-t6tmBr0Gxdhsk22mp9Pf3osO-SDsbvko6_2-fyJ3K-AQxs4tCrpMhw6pJWlDg5t4VCAQx0c2sKhcIFw6AIOdXA-k-npaDI4C5uKF2GMOcohi6WSWiVpwVVRlDwtjVZ9k5ZZXGaaFWmWJKhAKESWSilkAg2KK1nwSPMSvM0u2bCVNV8ILXUshCwicJgNuMTimMNtwSFix26SLnvkaP7YcrAo2CtpTfX0mPOMsSRlvEe6_mnmd174JBeo3sPE3tqv7pPNxRv1lWzUD0_mALoG_-BD0uEzceiY_gMWxU4K

Stöhr, J. R., Xiao, P.-G., & Bauer, R. (2001). Constituents of Chinese Piper species and their inhibitory activity on prostaglandin and leukotriene biosynthesis in vitro. *Journal of ethnopharmacology, 75*(2), 133-139. doi:10.1016/S0378-8741(00)00397-4

Stuart, D. L., & Wills, R. B. H. (2000). Alkylamide and Cichoric Acid Levels in Echinacea purpurea Tissues During Plant Growth. *Journal of Herbs, Spices & Medicinal Plants, 7*(1), 91-101. doi:10.1300/J044v07n01_11

Šutovská, M., Capek, P., Kazimierová, I., Pappová, L., Jošková, M., Matulová, M., . . . Gancarz, R. (2015). Echinacea complex – chemical view and anti-asthmatic profile. *Journal of ethnopharmacology, 175*, 163-171. doi:10.1016/j.jep.2015.09.007

Takahashi, S., Kubo, K., Waguri, S., Yabashi, A., Shin, H.-W., Katoh, Y., & Nakayama, K. (2012). Rab11 regulates exocytosis of recycling vesicles at the plasma membrane. *Journal of cell science, 125*(Pt 17), 4049-4057. doi:10.1242/jcs.102913

Todd, D. A., Gulledge, T. V., Britton, E. R., Oberhofer, M., Leyte-Lugo, M., Moody, A. N., . . . Cech, N. B. (2015). Ethanolic Echinacea purpurea Extracts Contain a Mixture of Cytokine-Suppressive and Cytokine-Inducing Compounds, Including Some That Originate from Endophytic Bacteria. *PLoS One, 10*(5), e0124276. doi:10.1371/journal.pone.0124276

Tsunozaki, M., Lennertz, R. C., Vilceanu, D., Katta, S., Stucky, C. L., & Bautista, D. M. (2013). A 'toothache tree' alkylamide inhibits Aδ mechanonociceptors to alleviate mechanical pain. *The Journal of physiology, 591*(13), 3325-3340. doi:10.1113/jphysiol.2013.252106

Tulleuda, A., Cokic, B., Callejo, G., Saiani, B., Serra, J., & Gasull, X. (2011). TRESK Channel Contribution to Nociceptive Sensory Neurons Excitability: Modulation by Nerve Injury. *Molecular pain, 7*(1), 30-30. doi:10.1186/1744-8069-7-30

Turcotte, C., Blanchet, M.-R., Laviolette, M., & Flamand, N. (2016). The CB2 receptor and its role as a regulator of inflammation. *Cellular and molecular life sciences : CMLS, 73*(23), 4449-4470. doi:10.1007/s00018-016-2300-4

Verdine, G. L., & Walensky, L. D. (2007). The Challenge of Drugging Undruggable Targets in Cancer: Lessons Learned from Targeting BCL-2 Family Members. *Clinical Cancer Research, 13*(24), 7264-7270. doi:10.1158/1078-0432.CCR-07-2184

Veryser, L., Bracke, N., Wynendaele, E., Joshi, T., Tatke, P., Taevernier, L., & De Spiegeleer, B. (2016). Quantitative In Vitro and In Vivo Evaluation of Intestinal and Blood-Brain Barrier Transport Kinetics of the Plant N-Alkylamide Pellitorine. *BioMed research international, 2016*, 5497402-5497402. doi:10.1155/2016/5497402

Veryser, L., Taevernier, L., Joshi, T., Tatke, P., Wynendaele, E., Bracke, N., . . . De Spiegeleer, B. (2016). Mucosal and blood-brain barrier transport kinetics of the plant N-alkylamide spilanthol using in vitro and in vivo models. *BMC Complement Altern Med, 16*, 177. doi:10.1186/s12906-016-1159-0

Wang, T., Ming, Z., Xiaochun, W., & Hong, W. (2011). Rab7: Role of its protein interaction cascades in endo-lysosomal traffic. *Cellular signalling, 23*(3), 516-521. doi:10.1016/j.cellsig.2010.09.012

Wei, X., Yang, B., Chen, G., Wang, D., Shi, Y., Chen, Q., & Kan, J. (2020). Zanthoxylum alkylamides improve amino acid metabolism in type 2 diabetes mellitus rats. *Journal of food biochemistry, 44*(10), e13441-n/a. doi:10.1111/jfbc.13441

Wu, L.-c., Fan, N.-c., Lin, M.-h., Chu, I.-r., Huang, S.-j., Hu, C.-Y., & Han, S.-y. (2008). Anti-inflammatory Effect of Spilanthol from Spilanthes acmella on Murine Macrophage by Down-Regulating LPS-Induced Inflammatory Mediators. *Journal of agricultural and food chemistry, 56*(7), 2341-2349. doi:10.1021/jf073057e

Yadav, V., Krishnan, A., & Vohora, D. (2020). A systematic review on Piper longum L.: Bridging traditional knowledge and pharmacological evidence for future translational research. *Journal of ethnopharmacology, 247*, 112255-112255. doi:10.1016/j.jep.2019.112255

You, Y., Ren, T., Zhang, S., Shirima, G. G., Cheng, Y., & Liu, X. (2015). Hypoglycemic effects of Zanthoxylum alkylamides by enhancing glucose metabolism and ameliorating pancreatic dysfunction in streptozotocin-induced diabetic rats. *Food & function, 6*(9), 3144-3154. doi:10.1039/c5fo00432b

Zandonadi, D. B., Matos, C. R. R., Castro, R. N., Spaccini, R., Olivares, F. L., & Canellas, L. P. (2019). Alkamides: a new class of plant growth regulators linked to humic acid bioactivity. *Chemical and biological technologies in agriculture, 6*(1), 1-12. doi:10.1186/s40538-019-0161-4

Zhai, Z., Liu, Y., Wu, L., Senchina, D. S., Wurtele, E. S., Murphy, P. A., . . . Cunnick, J. E. (2007). Enhancement of innate and adaptive immune functions by multiple Echinacea species. *Journal of medicinal food, 10*(3), 423-434. doi:10.1089/jmf.2006.257

Ziegler, J., Diaz-Chávez, M. L., Kramell, R., Ammer, C., & Kutchan, T. M. (2005). Comparative macroarray analysis of morphine containing Papaver somniferum and eight morphine free Papaver species identifies an O-methyltransferase involved in benzylisoquinoline biosynthesis. *Planta, 222*(3), 458-471. doi:10.1007/s00425-005-1550-4